

The 750keV INJECTOR UPGRADE PLAN

C.Y. Tan, D.S. Bollinger, W.A. Pellico & C.W. Schmidt

Date: July 7, 2010

Version: 07/07/10 09:42 AM

Table of Contents

Abstract.....	<u>1</u>
<u>1.</u> Introduction.....	<u>2</u>
<u>2.</u> The Plan.....	<u>2</u>
<u>3.</u> Analysis of Present Operations.....	<u>2</u>
<u>3.1.</u> Injector Downtime.....	<u>3</u>
<u>3.2.</u> Maintenance and Failures.....	<u>5</u>
<u>3.3.</u> Operating Costs.....	<u>5</u>
3.3.1. Power consumption.....	7
<u>3.4.</u> Future Expenditures.....	<u>7</u>
<u>4.</u> The Design.....	<u>9</u>
<u>4.1.</u> The H- Source.....	<u>9</u>
4.1.1. The HINS H- source at FNAL.....	10
<u>4.2.</u> Optics for the LEBT.....	<u>12</u>
4.2.1. Focusing with Xe gas.....	12
4.2.2. LEBT optics with 2 H- sources.....	13
4.2.3. The Solenoids.....	14
4.2.3.a. Magnetic stripping of H-	14
4.2.4. Chopper.....	17
4.2.4.a. The Einzel Lens.....	18
4.2.4.b. The Energy Pulser.....	20
<u>4.3.</u> The RFQ.....	<u>21</u>
<u>4.4.</u> Optics for the MEBT.....	<u>25</u>
4.4.1. Buncher.....	27
4.4.2. Quadrupoles.....	28
<u>4.5.</u> Layout.....	<u>30</u>
<u>5.</u> Performance Goals.....	<u>31</u>
<u>6.</u> Cost Estimate.....	<u>34</u>
<u>6.1.</u> Cost of RFQ.....	<u>36</u>
<u>7.</u> Conclusion.....	<u>37</u>
<u>8.</u> Acknowledgments.....	<u>37</u>
<u>A.1.</u> The BNL Injector.....	<u>38</u>
<u>A.1.1.</u> The BNL Injector (1982-1989).....	<u>38</u>
<u>A.1.2.</u> The BNL Injector (1989-present).....	<u>38</u>
References.....	<u>41</u>

Abstract

The present FNAL H- injector has been operational since 1978 and consists of a magnetron H-source and a 750keV Cockcroft-Walton Accelerator. The upgrade of this injector consists of replacing the present magnetron with a slit aperture and Cockcroft-Walton with a new magnetron with a round aperture and 200MHz RFQ. Operational experience from BNL (Brookhaven National Laboratory) has shown that a similar upgraded source and RFQ design will be more reliable and require less manpower to maintain than the present system.

1. Introduction

The present FNAL injector has been operational since 1978 and has been a reliable source of H- beams for the Fermilab program. At present there are two Cockcroft-Walton injectors, each with a magnetron H- source with a slit aperture [1]. Normally one source and Cockcroft-Walton is operational at any one time, with the other on stand by and ready to take over if there is a failure. With this two source operation, the injector has a reliability of better than 97%. However, issues with maintenance, equipment obsolescence, and retirement of critical personnel, have made it more difficult for the continued reliable running of the H- injector. The recent past has also seen an increase in both downtime and source output issues. With these problems which may already be here and those looming on the horizon, a new 750keV injector is being built to replace the present system. The new system will be very similar to the one at BNL (Brookhaven National Laboratory) which has a similar magnetron source with a round aperture and a 200MHz RFQ. This combination has been shown to be extremely reliable operationally [2].

2. The Plan

Based upon the experience at BNL and research/testing done at FNAL (HINS and source upgrade design studies) the plan is to replace the present injector with a round (dimpled) magnetron 35keV source followed by a 750keV RFQ. The design uses conventional technology such as solenoids, buncher cavity and steering elements to match into the present drift tube linac (DTL). For a small additional cost of adding a second magnetron, solenoid and steering elements, uninterrupted maintenance and repair can be carried out. The design intends to reuse as much of the present power sources, beam line hardware and infrastructure in order to keep cost at a minimum. New items which are required are a buncher cavity, three solenoids and a 1 to 1.5 m long RFQ and RF amplifier (beam pipe and the associated hardware will require mechanical labor), and three quadrupoles. This design uses two magnetrons (and their respective focusing solenoids) mounted on a slide, followed by a chopper, RFQ and buncher (diagnostics and miscellaneous hardware). The following paper will describe the present injector and its operations and cost followed by the a section which will describe in detail the design, physics and cost of the upgrade. For a comparison, an appendix is also included which looks at the BNL pre-injector system.

3. Analysis of Present Operations

The current Cockcroft-Walton accelerators have been a reliable source of protons to the FNAL complex for over 40 years. This reliability has been attained because of the combination of the two Cockcroft-Walton accelerators and a group of skilled technicians who have maintained the systems over the years. Continued improvements have been made over time, but the basic system has remained the same.

There has been extensive preventive maintenance done to reduce the chance of having an equipment related failure. Also the ion source and high voltage regulation have taken a fair amount of tuning, typically on a daily basis. All this effort has added up to a large number of “man hours” to

keep the systems running at an acceptable level. Figure 3.1 shows the beam output from the H- and I- sources over the past year. It can be seen from the histograms that the variations are large and thus require continuous tuning to meet the beam requirements for the downstream machines. The scale of the variation can be related to Booster turns where in this plot each bin is equivalent to approximately one Booster turn. For the rest of the analysis, the downtime logger, hand written log books, and the long time experience of the skilled technicians have been taken into account.



Figure 3.1: The variation in the H- (green) and the I- (red) sources over the past year. The large variation in intensity affects operations.

3.1. Injector Downtime

The injector systems are crucial for the operation of the accelerator complex. They supply all of the particles used for neutron therapy, p-bar and neutrino production, and Tevatron collider operations. When there is an equipment problem this leads to downtime for the entire complex. The downtime is logged by operations and this log has been searched through for injector downtime.

The total downtime for the injector over the past 9 years is about 300 hours. Figure 3.2 shows how the downtime is distributed over the injector systems.

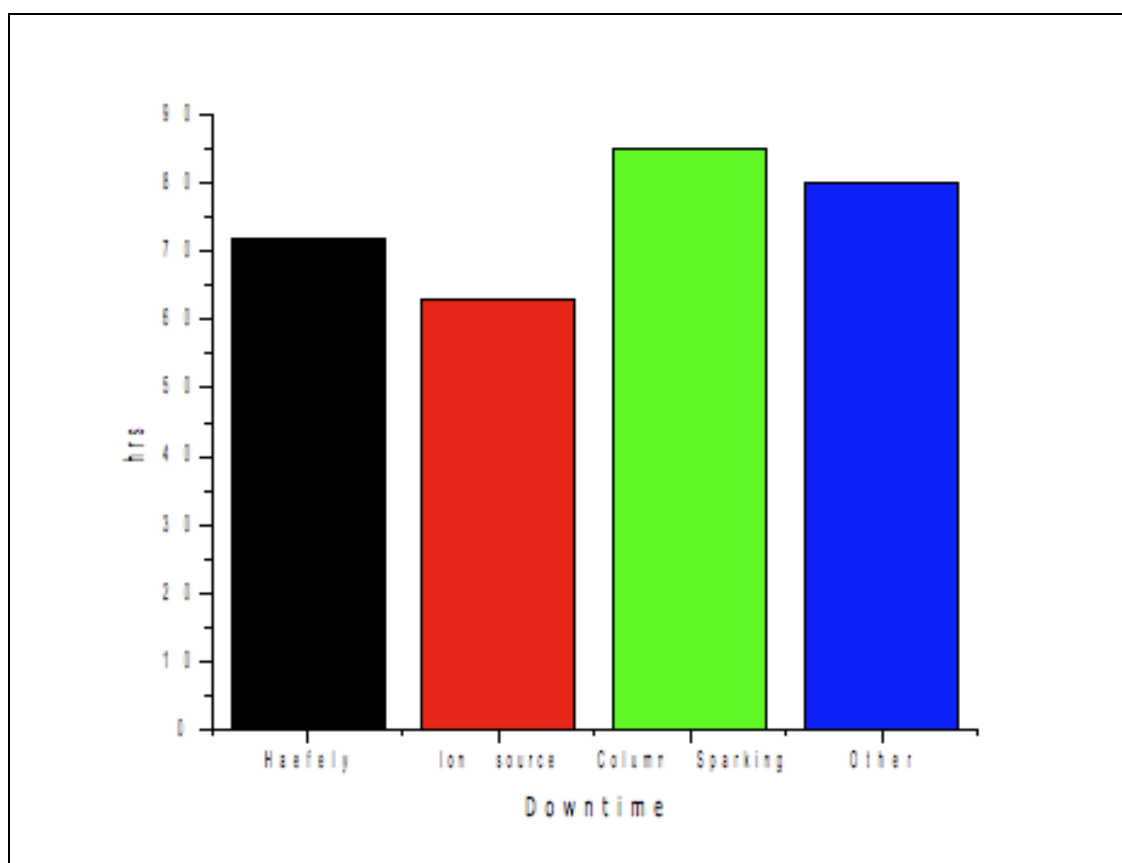


Figure 3.2: Downtime data in hours from Jan 2000 to the present.

The downtimes can be broken down in order of largest downtime first:

- i. Column This presents the largest amount of down time because of sparking in the Cockcroft-Walton accelerating columns which results in missed beam pulses during the spark and afterwards for the high voltage to recover.
- ii. Other These downtimes contain all the vacuum trips, repairs to elements in the 750keV line, switching to the backup H- source and other small problems.
- iii. Haefely The Haefely downtimes include the Haefely high voltage and its controls.
- iv. Source The ion source downtime is specific to the H- magnetron and associated electronics.

Since the Cockcroft-Walton consists of the Haefely and accelerating column they can be combined and shown as a percent of downtime. When this is done, the Cockcroft-Walton dominates and takes up about 52% of the total injector downtime. The breakdown of the downtimes in percent is shown in Figure 3.3.

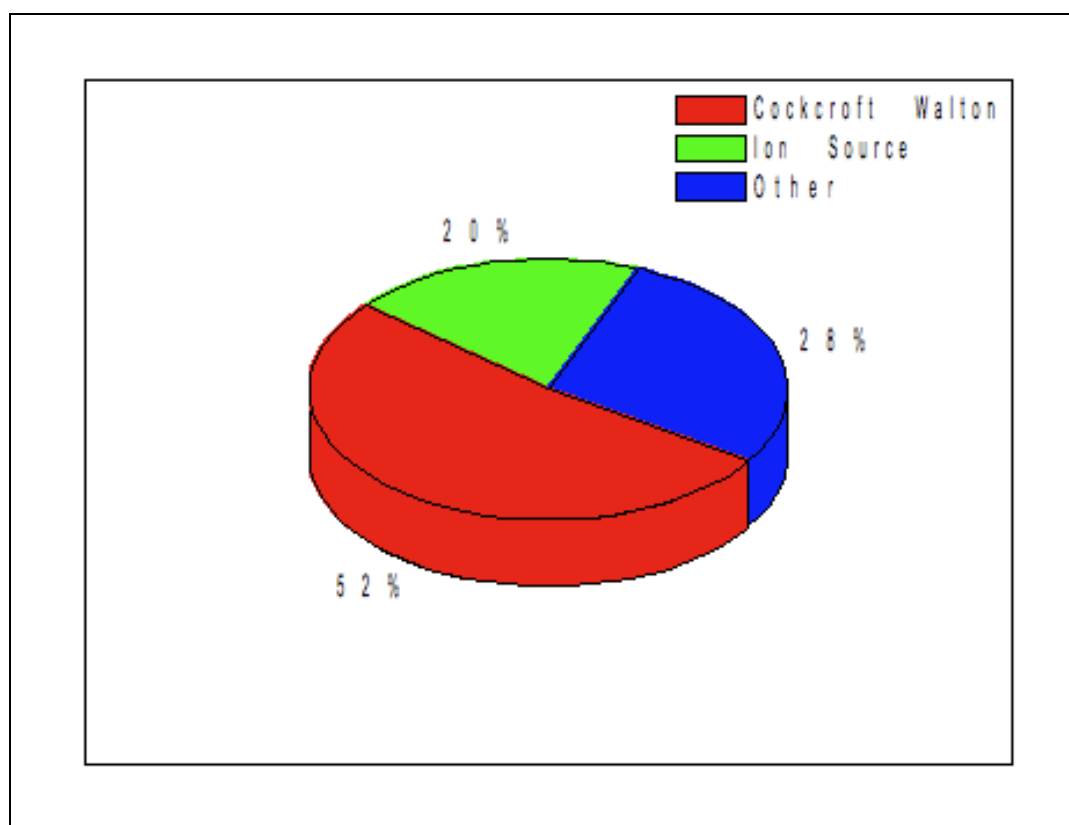


Figure 3.3: Percent of downtime by system. It is dominated by the Cockcroft-Walton.

Many of the failures associated with downtimes also lead to a loss of redundancy. This puts the injector at risk of not being able to deliver beam when needed.

3.2. Maintenance and Failures

There are several complex tasks associated with the maintenance of the injector systems. These activities include electrical, mechanical and chemical systems that take a special skill set that takes years to acquire. Table 3.1 shows some of the normal maintenance that takes place in the injector. With the exception of the power and extractor tubes the other items are preventive maintenance. There are many other tasks that are smaller and harder to quantify in a meaningful way.

3.3. Operating Costs

The actual cost of operating any system includes the number of man hours worked, cost of equipment, and power consumption among other factors. The Cockcroft-Walton accelerators require a large number of man hours coupled with a few high dollar maintenance items. The Pre-Acc group currently consists of 2 technicians, 2 Sr. Operations Specialists, and 2 Engineering Physicists. One of the Engineering Physicists is currently working on numerous other projects and will not be included in the following discussion. Figure 3.4 shows the percentage of man hours worked by full time employees on the injector systems and all other projects. The operations

specialists **are a few months away from retirement** so the distribution of man hours will change in the near future.

There are numerous costs associated with the equipment itself. Some of the bigger material costs are listed in Table 3.2. The labor to perform these far outweighs the material costs. For example the ion pump rebuild requires about 120 man hours and the generator rebuild takes about 32 man hours to remove and reinstall.

Maintenance Item	Interval	Labor (man hours)
Generator Brushes		
Checking	Monthly	2
Replacing	Weekly	2
Water Resistor		
Flushing	Monthly	4
Changing	Annually	8
Ion Source		
Cleaning	Quarterly	16
Tuning	Daily	4
Cesium		
Change Boiler	Annually	8
Ion Pump		
Zapping	Quarterly	2
Change	Annually	80
Power Tubes	Biennially	4
Extractor Tubes	Annually	1
Interlock Testing	Annually	16
Clean Cold Box/Diaphragm	Annually	80

Table 3.1: Estimate of the man hours needed to keep the injector running.

Work	Cost
Generator rebuild	\$2.8k
Ion pump rebuild	\$5k
Cockcroft-Walton pits cleanse	\$5k

Table 3.2: *The big material costs.*

3.3.1. Power consumption

Each Cockcroft-Walton consumes about 45 kW of electricity. There is also a significant heat load from the quad power supplies. The present operating parameters of the slit source+Cockcroft-Walton is summarized in Table 3.3.

Parameter	Value	Units
H- current	50 – 60	mA
Extraction voltage	18	kV
Arc voltage	140 – 160	V
Arc current	40 – 60	A
Repetition rate	15	Hz
Pulse width	80	μ s
Duty factor	0.12	%
rms normalized emittance	$\epsilon_x=0.23, \epsilon_y=0.27$	$\pi \cdot \text{mm} \cdot \text{mrad}$
Cs consumption	0.5	mg/hr
Average power	$150 \text{ V} \times 50 \text{ A} \times 15 \text{ Hz} \times 80 \mu\text{s} = 9$	W

Table 3.3: *Operating parameters of the present injector.*

3.4. Future Expenditures

Table 3.4 lists a set of possible future upgrades to the Haefely controls, ion source support electronics and the needed spares. The cost estimate for the ion source electronics upgrades are based on the HINS project designs.

With the impending retirement of the resident Cockcroft-Walton experts, there is a certain amount of risk that significant downtime will occur. Currently technicians are being trained to replace the experts, however the loss of 82 years of experience will take some time to recover.

Project	Cost
Haefely HV regulator	unknown
Spare anode power supply	\$22k
Spare chopper power supply	\$6k
Source heaters DC power supplies	\$9k
Source extractor pulser	\$6k
Ground vacuum turbo pump	~\$30k

Table 3.4: Future cost to maintain the injector hardware.

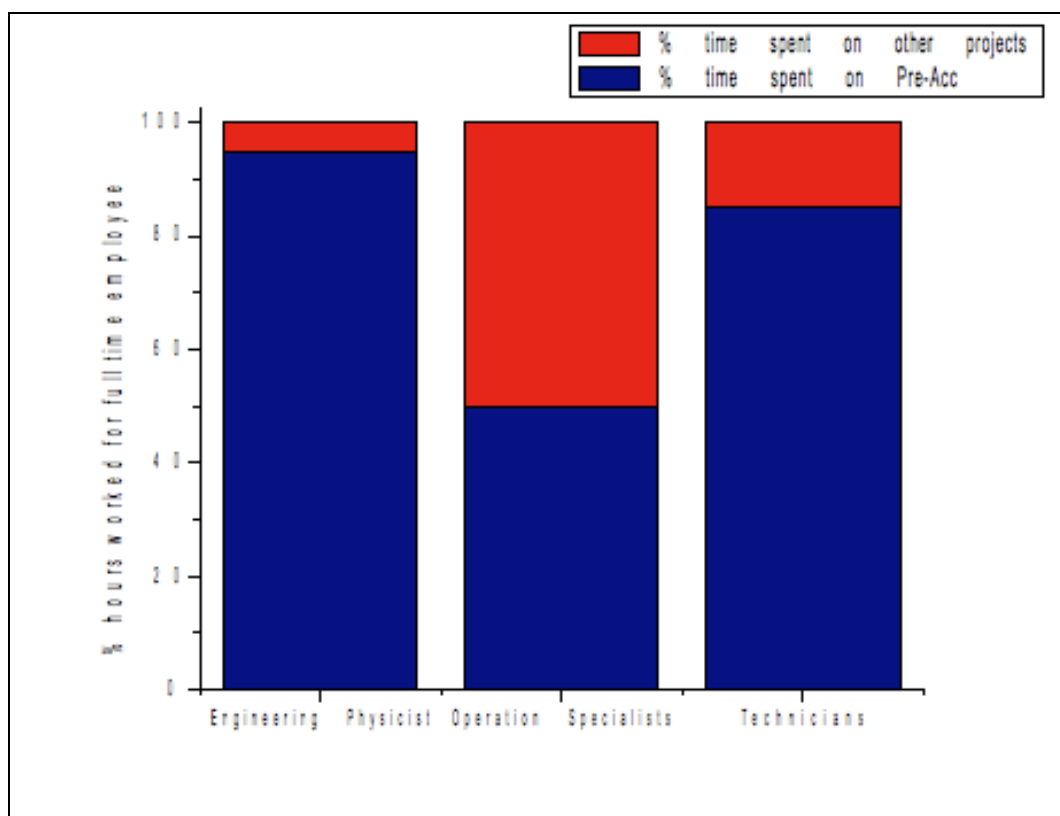


Figure 3.4: The breakdown of hours worked by the full time employees of the Pre-Acc group.

4. The Design

The design can be divided into two transport lines: the low energy beam transport (LEBT) and the medium energy beam transport (MEBT). The LEBT is the transport line before the RFQ and the MEBT is the transport line from the end of the RFQ to the beginning of the DTL.

For the LEBT, the proposed design will contain two H- magnetron sources for increased reliability. Each H- magnetron source will be the round type and will be mounted on a slide. (See Figure 4.4). The beam out of the source is at 35keV and should be > 60 mA and thus space charge dominated. Therefore, it must be focused with a solenoid right out of the source to preserve its emittance. The paraxial beam is transported through a short beam line to one more solenoid which strongly focuses it into the small aperture (1.8 cm in radius) at the entrance of the RFQ. Xe gas will also be used for neutralizing and focusing the H- beam because it has been shown at BNL that there is an increased transmission efficiency when Xe gas is used [3]. A low energy chopper which consists of an Einzel lens near the entrance of the RFQ and a voltage pulser designed into the H- source will be installed in the LEBT because it is much easier to chop the beam at low energy and also there is insufficient space in the MEBT. It is necessary to have this combination chopper design because a pure electrostatic kicker will de-neutralize the H- and any advantage of Xe gas focusing will be lost during the chopping process [4].

The RFQ will focus, bunch and accelerate the H- beam from 35keV to 750keV. Once the beam exits the RFQ it has a tendency to blow up both longitudinally and transversely and thus the MEBT must be short and must contain quadrupoles and a buncher. The proposed MEBT is a copy of the BNL MEBT which is < 75 cm long and contains 3 quadrupoles and one two gap buncher.

Using both empirical data and computer simulations, it is predicted that about 65% of the beam can be transported from the H- source to the end of the first DTL. If the source can produce 60 mA of H- beam (Note: the BNL source routinely produces 90 – 100 mA of H- beam [2]), it is predicted that 37.5 mA will be at the end of the first DTL. For a comparison, the present Cockcroft-Walton system transports 37.5mA to the end of the first DTL for a source current of ~ 60 mA. See Figure 5.1.

4.1. The H- Source

FNAL has been using an H- magnetron ion source for ~ 34 years and as such has accumulated much experience and equipment associated with this source. Following the initial FNAL use, ANL (Argonne National Laboratory), DESY and BNL have also adopted this source design to produce H- beams for injection into their linacs. Originally, the source had a slit aperture producing a ribbon shaped beam which was transformed to an elliptically shaped beam which could be further accelerated, transported and injected into a linear accelerator. BNL improved it using a circular aperture to produce a round beam which could be more easily focused and injected into an RFQ. Recently, a source, very similar to the BNL source, was built and tested at FNAL for the HINS R&D program.

The recent work to produce a circular-aperture direct-extraction H- source for the HINS project is conveniently applicable to a source for this plan. Likewise, two sources which have been received from Argonne recently due to the dismantling of the Intense Pulsed Neutron Source (one was loaned to them many years ago and the second ANL built as a spare) has given many significant parts for assembling the sources needed for this plan. This will greatly reduce the effort, cost and time to have a working source for the RFQ tests and operation.

Like most accelerator equipment the H- source is operated at or near its maximum output and thus has a variable and limited lifetime (a good life time is about 3 to 4 months) so that it requires much maintenance and cleaning with frequent tuning during operation. To have high reliability from such an injector, it is very desirable to have two sources, one operating and one as backup, feeding the next device.

With the experience this source has had at FNAL and elsewhere it is a logical choice to use it for this plan. The low duty-factor (0.2%), modest intensity (50 to ~100 mA), pulsed (15 Hz) H- ion source of the magnetron surface-plasma type is suitably matched to the capabilities of the present FNAL Linac and Booster to meet the objectives of the FNAL program. It is not in the same league with the high current and high duty-factor modern H- sources which are used to produce intense secondary beams. Still, with proper attention and the manpower to maintain it, the magnetron source has and can continue to meet the capacity of the FNAL Linac and Booster.

4.1.1. The HINS H- source at FNAL

A round source has been built at FNAL specifically for the HINS program. The physical geometry of the HINS source is nearly the same as the source used in this plan although the operating specifications for the HINS source are quite different than for the proposed source. Table 4.1 compares some of the parameters of the two sources and Figure 4.1 shows the cathode surface with the dimple which is the same for both sources.

Parameter	Initial HINS	Proposed Source	Units
Beam energy	50	35	keV
Beam current	20	> 50	mA
Pulse length	1000	120	μ s
Repetition Rate	2 – 5	15	Hz

Table 4.1: A comparison of the H- source parameters for HINS [5] and the proposed source. The complete parameters of the proposed source which should be similar to the BNL source are shown in Table A1.1.

The measured emittances for the HINS H- source are $\epsilon_{h, \text{norm}} = 0.61 \pi \text{ mm} \cdot \text{mrad}$ and $\epsilon_{v, \text{norm}} = 1.13 \pi \text{ mm} \cdot \text{mrad}$ for 90% of the beam are shown in Figure 4.2. Although the vertical emittance is ~40% larger than the horizontal emittance, due to a transverse source magnetic field, both are rather small and within limits of the HINS RFQ design.

For the proposed source, the parameters more closely follow that of the BNL source (except for the repetition rate, pulse width and average power) and is summarized in Table A1.1.

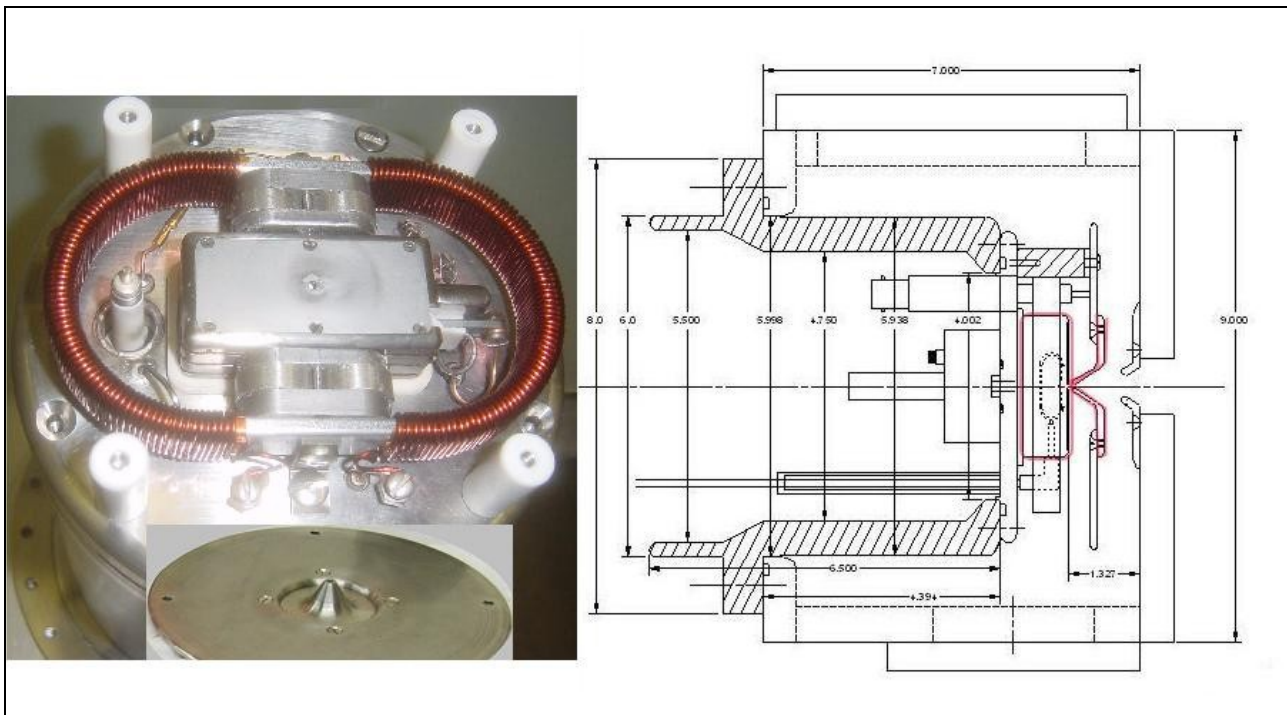


Figure 4.1: The picture on the left is the direct-extraction H-magnetron ion source with extraction electrode shown in the inset. The drawing on the right shows how the ion source is assembled in the enclosure. The parts in the picture are highlighted in red in the drawing.

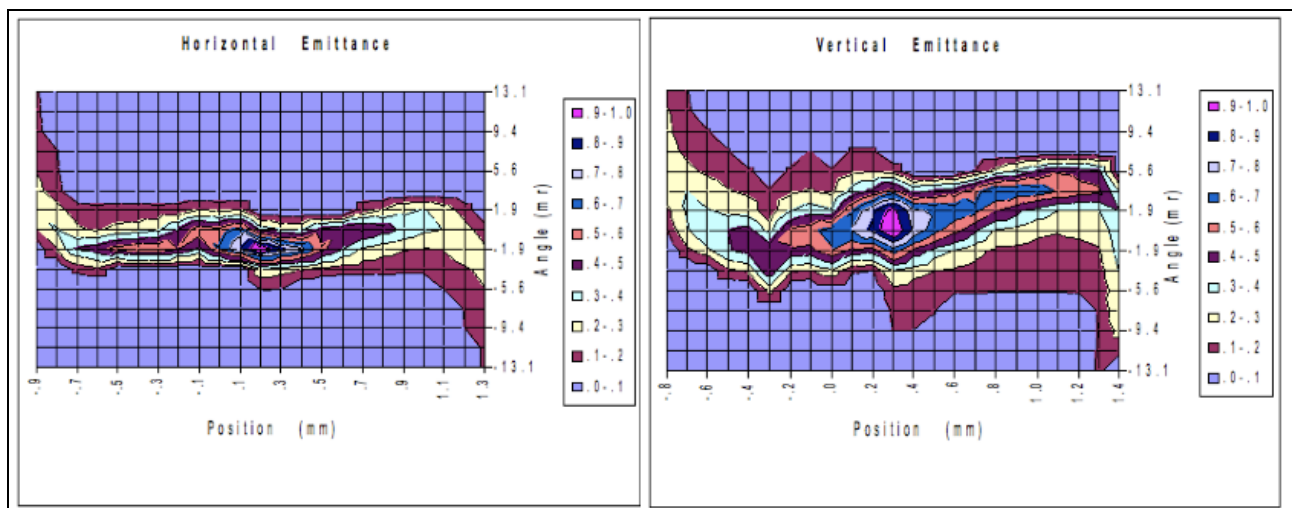


Figure 4.2: The HINS source parameters in this measurement are 50keV energy, 20 mA current and 11 kV extraction voltage. The measured normalized, 90% emittances at the output are $\epsilon_{h, \text{norm}} = 0.61 \pi \text{ mm} \cdot \text{mrad}$ and $\epsilon_{v, \text{norm}} = 1.13 \pi \text{ mm} \cdot \text{mrad}$.

4.2. Optics for the LEBT

The H- beam from the source is space charge dominated and at low energy its emittance will blowup if there is insufficient focusing. The combination of gas focusing and solenoid focusing will enable the transport of the H- beam with smaller losses to the entrance of the RFQ than without gas focusing. However, care must be used with gas focusing because if the gas pressure is too high or the transport length is too long, stripping of the H- ions will become a problem. Furthermore, if an electrostatic chopper is used for low energy chopping, the Xe ions used in gas focusing will be swept away by the electric field if it is turned on for too long. The solution to this problem is to use a combination of an Einzel lens placed close to the entrance of the RFQ to act as a mirror for the H- ions for the front edge of the beam pulse and to lower the energy of the H- source at the back edge of the beam pulse so that the RFQ will not accept the beam. Section 4.2.4. will have a full discussion of this combination.

4.2.1. Focusing with Xe gas

The idea behind gas focusing is completely described by Reiser [6]. When low pressure Xe is introduced, one or both electrons can be stripped from the H- ions to form either H⁰ or H⁺ ions, and Xe can form Xe⁺ ions and electrons. The electrons are repelled by the H- beam to the wall while the H⁺ and Xe⁺ ions are trapped in the H- beam region. The H⁺ and Xe⁺ ions attract and focus and neutralize the H- beam. The gas that is used is Xe because its high atomic mass (131.3 amu) keeps the escape velocity of the Xe⁺ ions low and so keeps the Xe⁺ ions trapped.

A crude calculation which assumes that when the H- is over-neutralized, the amount of focusing of H- from the Xe⁺ ions, independent of beam current, is (Eq. 4.308 of Reiser [6])

$$a = 1.74 \times 10^5 \epsilon_n \frac{1}{(V_b V_i)^{1/4}} \quad (1)$$

where $\epsilon_n = (0.15 \times 10^{-5}) \pi \text{ m} \cdot \text{rad}$ or $1.5 \pi \text{ mm} \cdot \text{mrad}$ (using $5 \times$ rms emittance, see Table 4.3) is approximately the output emittance of the H- source, $V_b = 35 \text{ kV}$ is the potential difference applied to the H- beam, $V_i = 12.1 \text{ V}$ is the ionization potential of Xe when the H- beam goes through Xe gas and a is the radius of the focused beam. Putting in these numbers, the radius of the focused H- beam is $a = 3.2 \text{ cm}$ (1.25") and thus implies that the beam pipe must be at least 2.5" in diameter.

In fact, BNL has demonstrated that using low pressure Xe gas at 3.7×10^{-6} torr, the transmission efficiency of H- from the source to the entrance of the RFQ is improved by 30% over optics without the Xe gas [3]. Therefore, it is important to use Xe gas in the FNAL LEBT. However, since Xe does strip some H-, some intensity will be lost. The following is a simple formula which relates the fractional loss per unit length λ of H- to the molecular density $\rho [\text{m}^{-3}]$ of Xe in the beam pipe and ionization cross section $\sigma [\text{m}^2]$ of Xe:

$$\lambda = \rho \sigma \quad (2)$$

and for the proposed LEBT, at $\rho = (3.3 \times 10^{22}) \times (3.7 \times 10^{-6} [\text{torr}]) = 1.2 \times 10^{17} \text{ m}^{-3}$ 20°C [7] and for $\sigma = 3 \times 10^{-19} \text{ m}^2$ 35keV H- ions impacting on Xe [8], the fractional number of H- lost per meter is $\lambda = 0.036$. The LEBT is about 2 m long, so about 7% of the H- will be lost from gas stripping. Note: BNL measured 32% of H- loss from Xe gas stripping (and 20% loss by using Eq. (2)) for their 4 m long LEBT [3]. Therefore, it can be expected that gas stripping for a 2 m long LEBT can

be as high as 16%, i.e. a factor of two larger than the back of the envelope calculation shown above.

Another consideration is that it takes a finite time for neutralization to take place. BNL has measured it to be about $40\mu\text{s}$, so the pulse length must be increased by this amount, i.e. if the pulse length is $120\mu\text{s}$, then only the last $80\mu\text{s}$ is useable.

4.2.2. LEBT optics with 2 H- sources

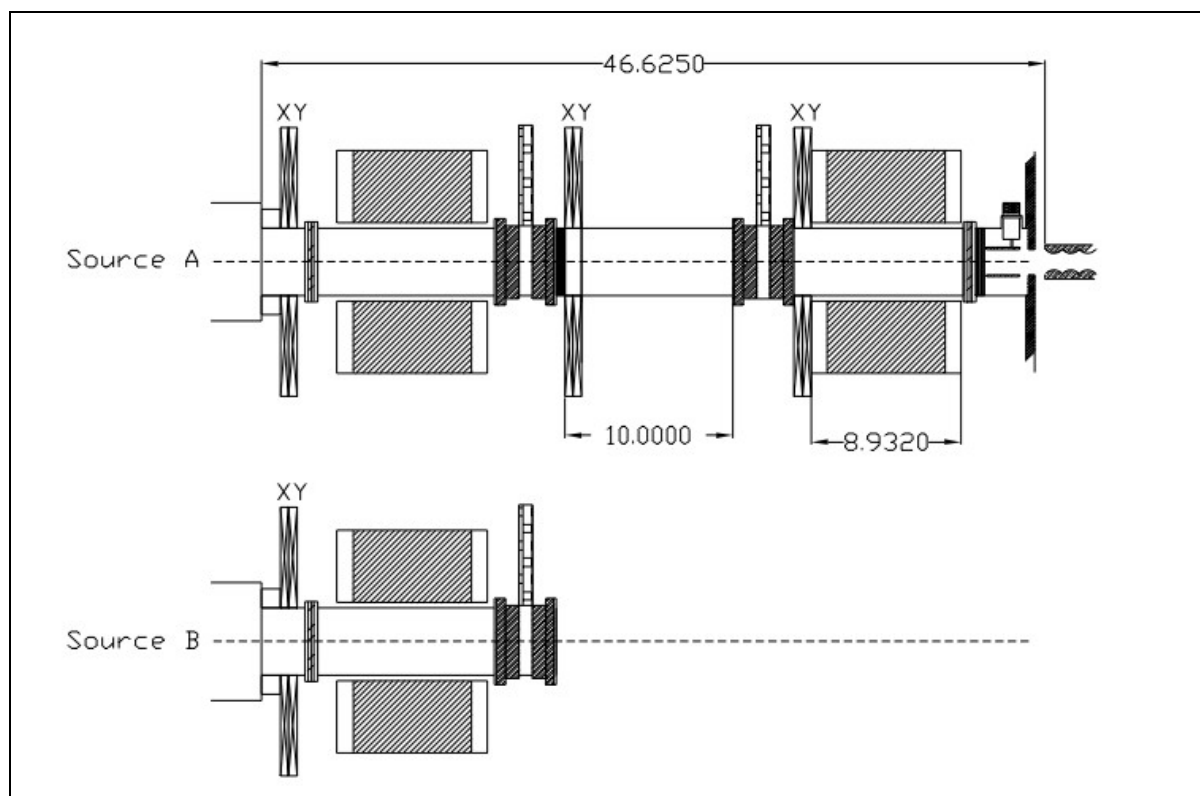


Figure 4.3: The LEBT (drawn to scale) has 2 H- sources but only one is used at any given time. The two sources are mounted on a slide so that either source can be slid into operation. A more detailed drawing with the slide is shown in Figure ??.

The LEBT has been designed with two H- sources to ensure high reliability. Figure 4.3 shows a possible layout of the LEBT with source A as the operational source. Both source A and B are mounted on a slide so that either source can be slid into the injection line for operations. A 10" space has been deliberately left for the installation of beam instrumentation and a pump port. Note: the lengths of the LEBT shown in Figure 4.3 are only guides for the final design because the instruments which occupy the 10" space will probably take less space than what has been reserved.

The strength of the solenoids have been calculated with Trace2D from the source to the entrance of the RFQ. The results are summarized in Table 4.2. Figure Error: Reference source not found is the Trace2D result.

Trace2D Element ID	Element Type	Value
2	Solenoid	2313 G
4	Solenoid	2496 G

Table 4.2 Summary of the relevant parameters used to match a DC H- ion beam from the source to the entrance of the RFQ for source A and B configurations See Figure Error: Reference source not found for the Trace2D element ID.

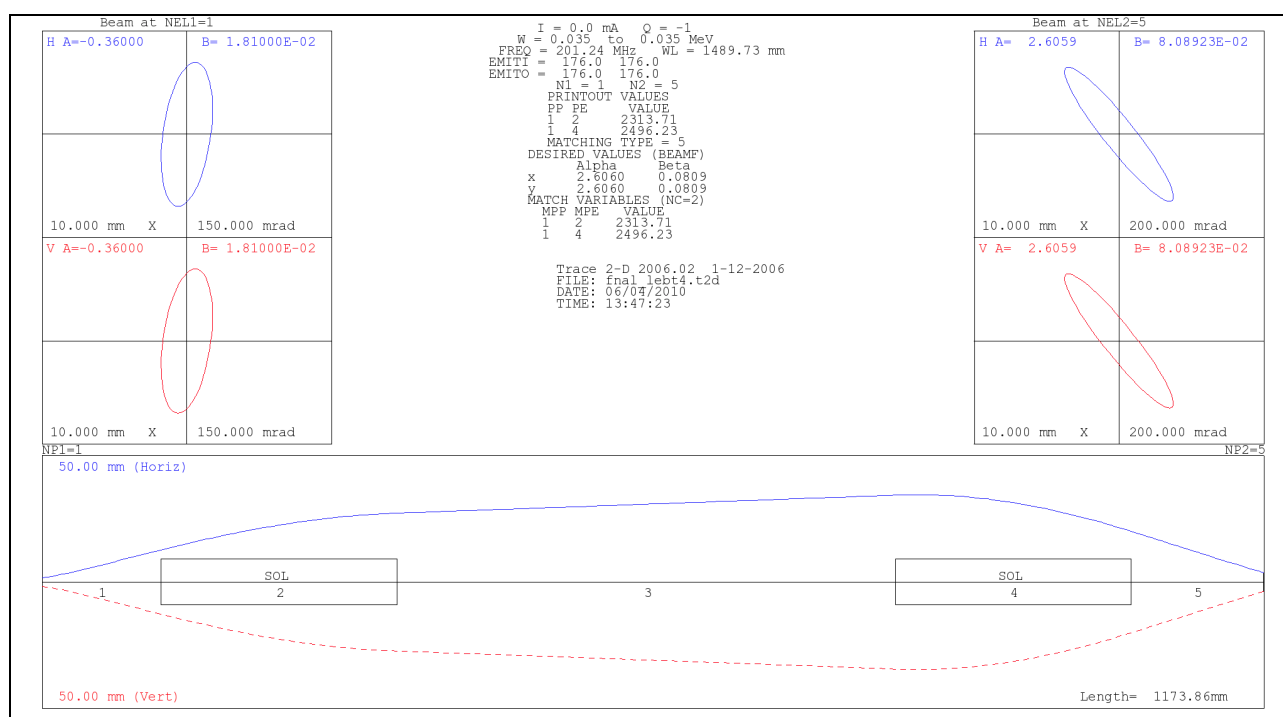


Figure 4.4: The optics of the LEBT for zero current H- beam from the source to the entrance of the RFQ. The solenoidal fields are less than 2500 G.

4.2.3. The Solenoids

V. Kashikhin has designed and simulated the magnetic properties of the solenoids which are compatible with the optics simulations. A longitudinal cross sectional view of the solenoid is shown in Figure 4.5. Compared to the BNL solenoid, this solenoid is shorter by about 1.5" but keeps the same outer radius. The bore radius, however, has been increased from 4.255" to 4.75" so that there is space to align the axis of the 4" beam pipe to the magnetic axis of the solenoid. The flux lines and the flux density along the longitudinal axis at zero radius are shown in Figure 4.6.

4.2.3.a. Magnetic stripping of H-

B-fields can strip H- because the two electrons and the proton of the H- experience opposite Lorentz forces. The energy required to strip the loosely bound electron is only 0.75 eV, while in contrast it is 13.6 eV for the tightly bound one. However, for the magnetic fields and energy of the H- in the LEBT magnetic stripping is irrelevant. A quick calculation below will show that this is

indeed the case.

When the B-field in the laboratory frame is boosted to the frame of 35keV H- ions, the H- ions will see an E-field $\vec{E} = \gamma(\vec{v}/c) \times \vec{B}$, which in more convenient units is

$$E [\text{MV/cm}] = 3.197 p [\text{GeV}/c] B [\text{T}] \quad (3)$$

where p is the momentum of the H- in the laboratory frame. The only source of B-field in the LEBT are from the solenoids. The solenoidal field is about 0.25T in the LEBT design. For 35keV H- ions, the momentum is $p = 8.1 \text{ MeV}/c$, and by using Eq. (3), the E-field for $B=0.2\text{T}$ in the rest frame of the H- ion is re $E = 6.5 \times 10^3 \text{ V/cm} \ll 10^6 \text{ V/cm}$ quired for the weakly bound electron to tunnel through the potential barrier [9]. In fact, the present H- source has a 90° bend which has a B-field of 0.25 T and there has been no noticeable H- loss. Therefore, the largest contributor to H- stripping is from the background gas (see section 4.2.1.) and not from the magnetic field.

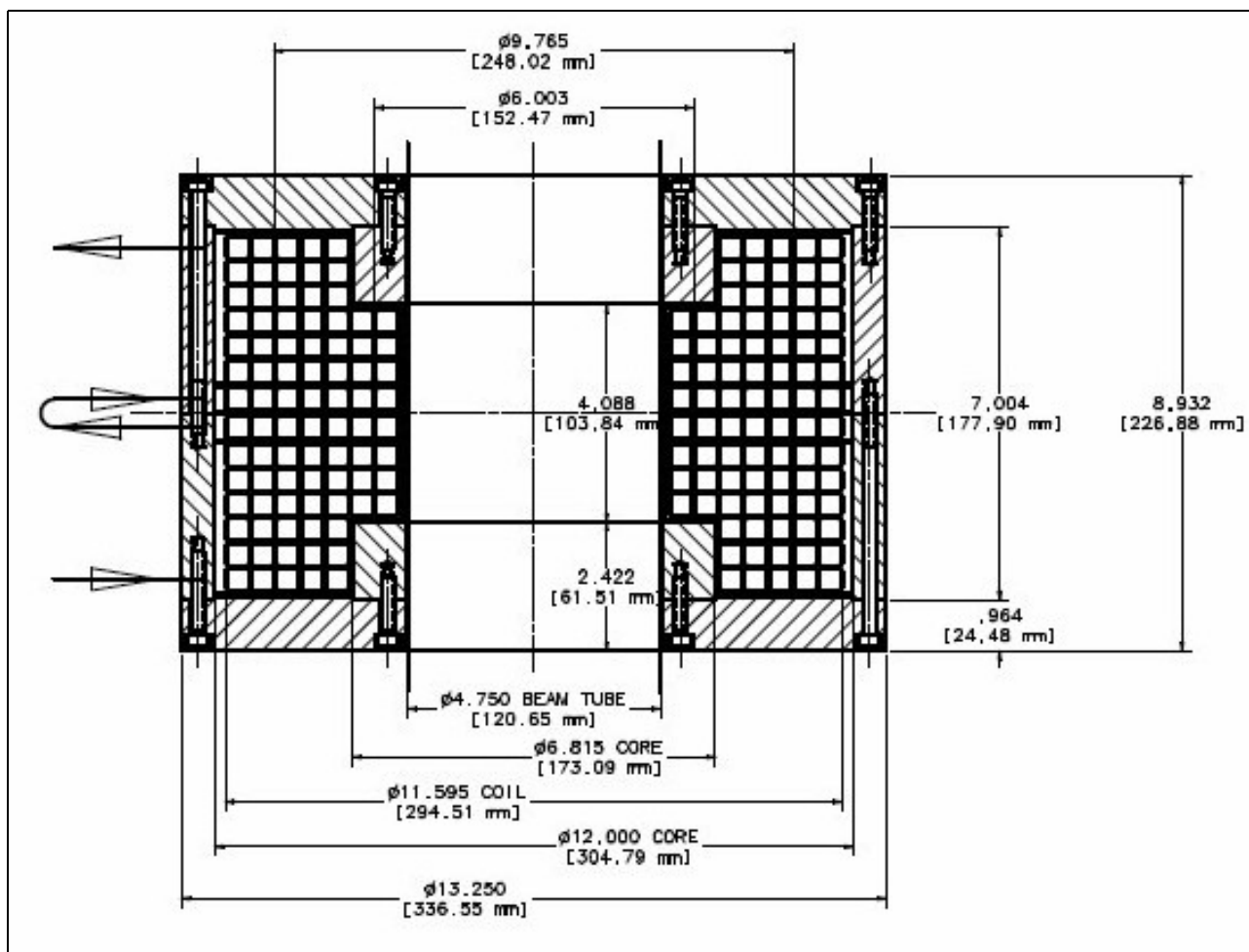


Figure 4.5: This is a longitudinal cross sectional view of the solenoid design. It is much more compact than the BNL solenoids. (Designed by V. Kashikhin)

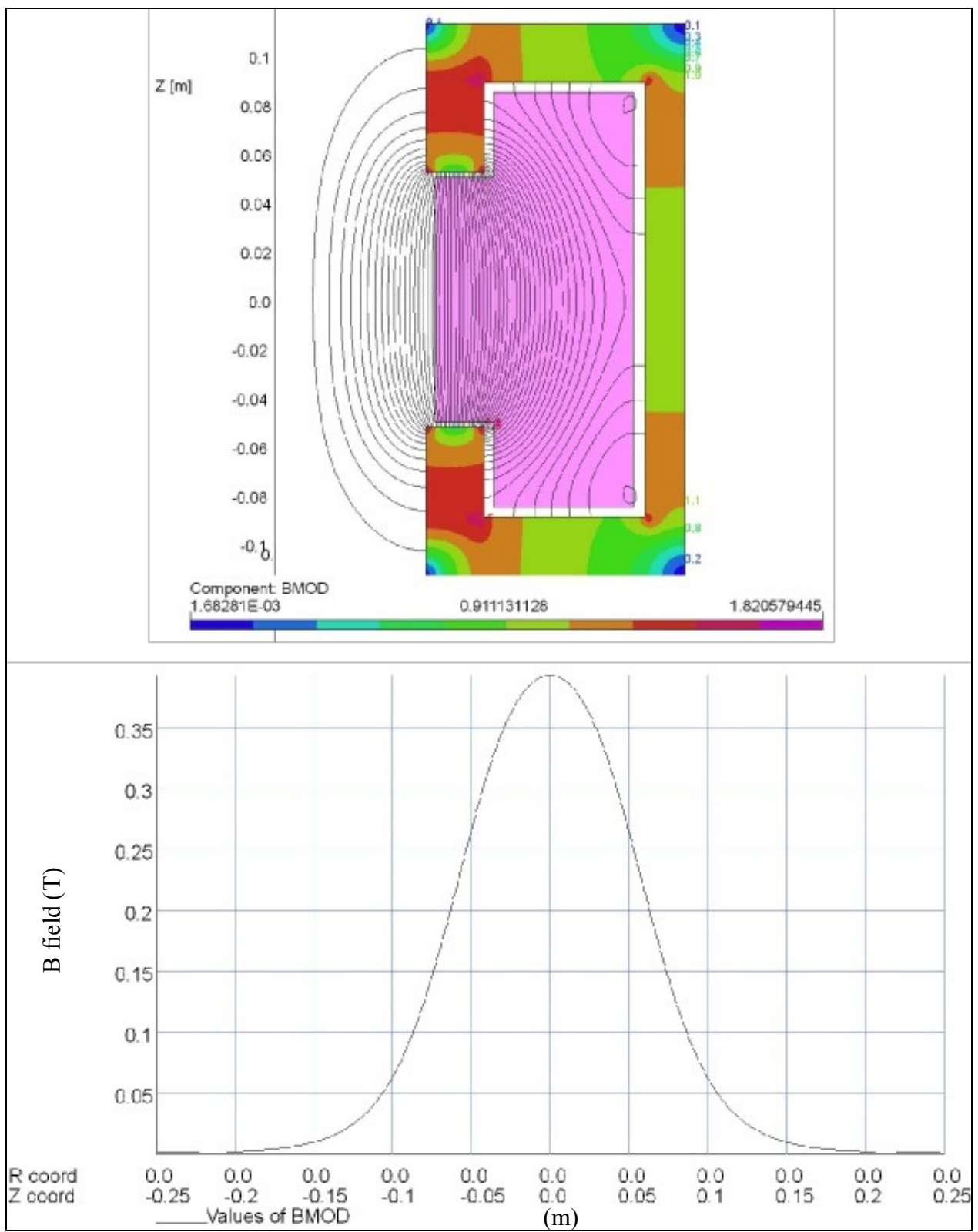


Figure 4.6: The upper figure shows the magnetic flux lines of the solenoid and the bottom figures shows the magnetic flux along the longitudinal axis of symmetry. $z=0$ is at the centre of the solenoid.

4.2.4. Chopper

The chopper is in the low energy part of the injector and so some care must be taken in the design, operation and placement of the chopper from the BNL experience. If electrostatic choppers (which use parallel plates) are used and the voltage on the plates is on for a long time ($\gg 1 \mu s$), the H- emittance grows because the neutralizing Xe ions are swept out of the H- beam. Fortunately, from studies done at BNL [4], de-neutralization is confined in the region between the chopper plates.

A possible solution for the de-neutralization problem is to use a magnetic chopper. The reason why magnetic choppers do not de-neutralize the H- beam is because the force on the Xe+ ions is small.¹ However, a magnetic kicker has not been chosen for the chopper because of the following reasons:

1. A magnetic kicker will require a ceramic beam pipe because of the fast rise and fall times required.
2. The instantaneous power required for a 10" long magnet placed at the location reserved for 10 inches of instrumentation shown in Figure 4.3 is in the MW range.
3. For neutralization purposes, it is much better to place the magnetic kicker as close as possible to the entrance of the RFQ. However, the final focusing solenoid is in the way.

A better solution for the chopper is a combination of an Einzel lens and an energy pulser designed into the H- source. The Einzel lens is placed as close as possible to the entrance of the RFQ so that when the Einzel lens is turned on, the Einzel lens acts like a mirror and reflects the 35 keV H- ions from the entrance of the RFQ. Unfortunately, the Einzel lens cannot work alone because its PFN (pulse forming network) which powers the Einzel lens cannot recharge within $\sim 100 \mu s$ after it discharges and so another device is required to shut the H- beam off. The solution is an energy pulser which forms the second half of the chopping system. The pulser in the H- source reflects the H- beam coming out of the source so that none escapes.

For example, the combination chopper works as follows for neutron therapy (See Figure 4.7):

1. The Einzel lens stops the first $\sim 40 \mu s$ of the H- beam from entering the RFQ because it takes this amount of time for the H- beam to be fully neutralized in the LEBT. The energy pulser is off at this time.
2. The Einzel lens is turned off by firing a thyatron to short its voltage to ground and the H- beam goes into the RFQ. Both the Einzel lens and the energy pulser are off for $60 \mu s$ which is the required bunch length for neutron therapy.
3. The energy pulser is turned on by firing its thyatron which sets its voltage to -36.5 kV. The potential difference between the source and the electrode/plate is now at kV -1.5 which is sufficient to repel the H- beam.
4. The H- source turns off, the capacitors of the PFNs which power the Einzel lens and the pulser charge back up and the combination chopper is ready to chop the beam again in $1/(15[\text{Hz}])=67 \text{ ms}$.

¹ The speed of the Xe+ ions are small compared to the H- ions and so $|\vec{v} \times \vec{B}|$ is much smaller than the equivalent E field for the same kick on the H- ions.

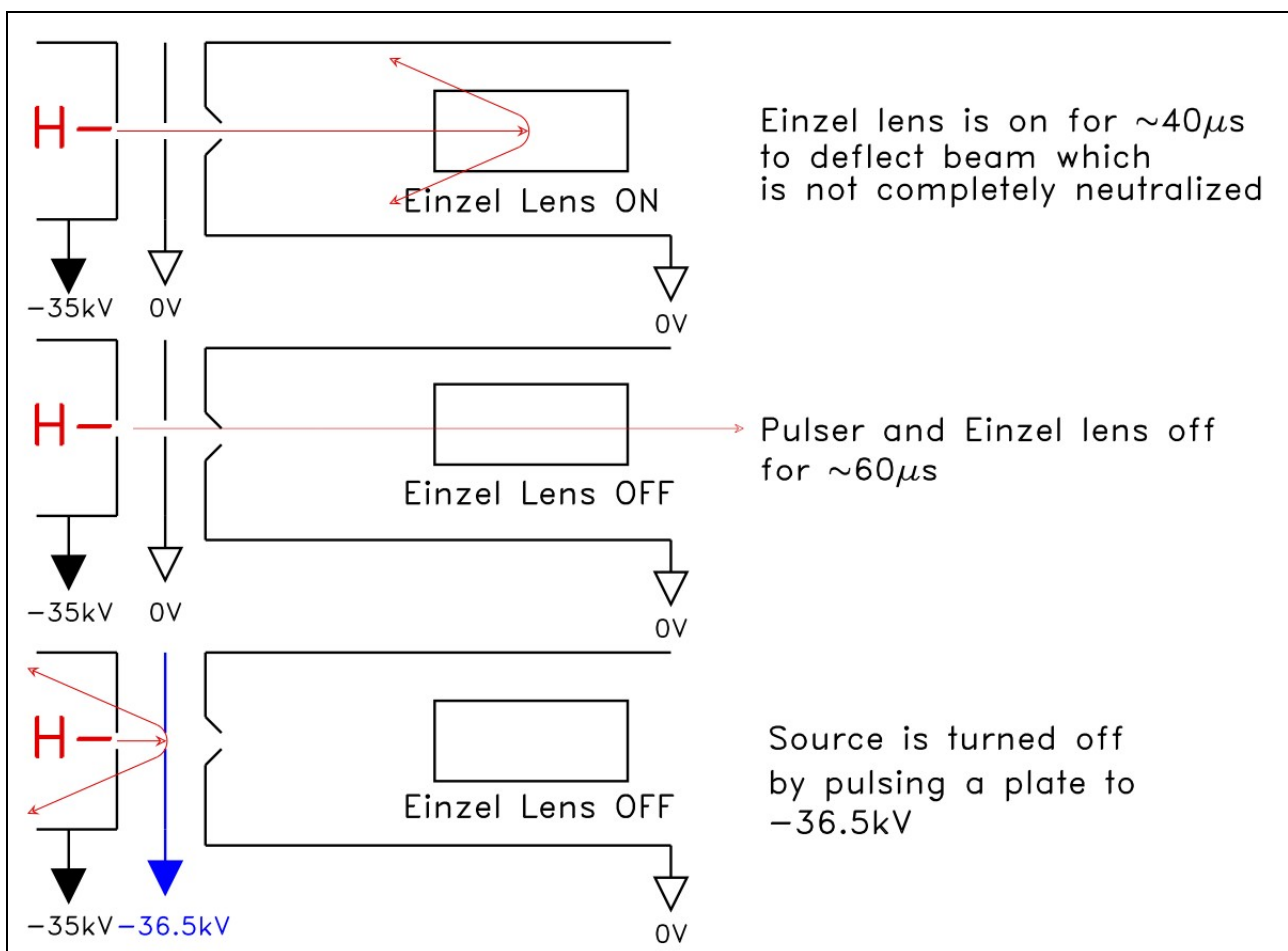


Figure 4.7: The chopper is a combination of an Einzel lens and a energy pulser. In this example which is used for neutron therapy, the H- source is turned on and the first $40\mu\text{s}$ of the H- beam is not transmitted into the RFQ because it takes this amount of time to neutralize the H- beam. Everything is off for the next $60\mu\text{s}$ so that the neutralized beam is sent into the RFQ. After $60\mu\text{s}$ the beam is turned off by the energy pulser. The cycle repeats after $1/15[\text{Hz}]=67\text{ms}$ when the PFNs have recharged and the H- source can be turned on again.

4.2.4.a. The Einzel Lens

The Einzel lens is placed as close as possible to the entrance of the RFQ in order to keep the de-neutralized region as small as possible when the Einzel lens is on. Computer simulations with SIMION have shown that the optimal length and diameter of the Einzel lens to be 2" and 1.5" respectively. Figure 4.8 shows how the H- beam is reflected at the Einzel lens calculated by SIMION. When the Einzel lens is on at -36 kV all the incident H- beam is reflected away from the entrance of the RFQ. When the Einzel lens is off, the H- beam is transmitted into the RFQ. The capacitance of the Einzel lens in the structure calculated with SIMION shows that it is $\ll 10\text{ pF}$ and so can be discharged very quickly in $< 1\text{ ns}$ if the resistance of the discharge circuit $< 50\Omega$.

Figure 4.9. shows a possible design of the mounting for the Einzel lens at the end of the LEBT and before the RFQ.

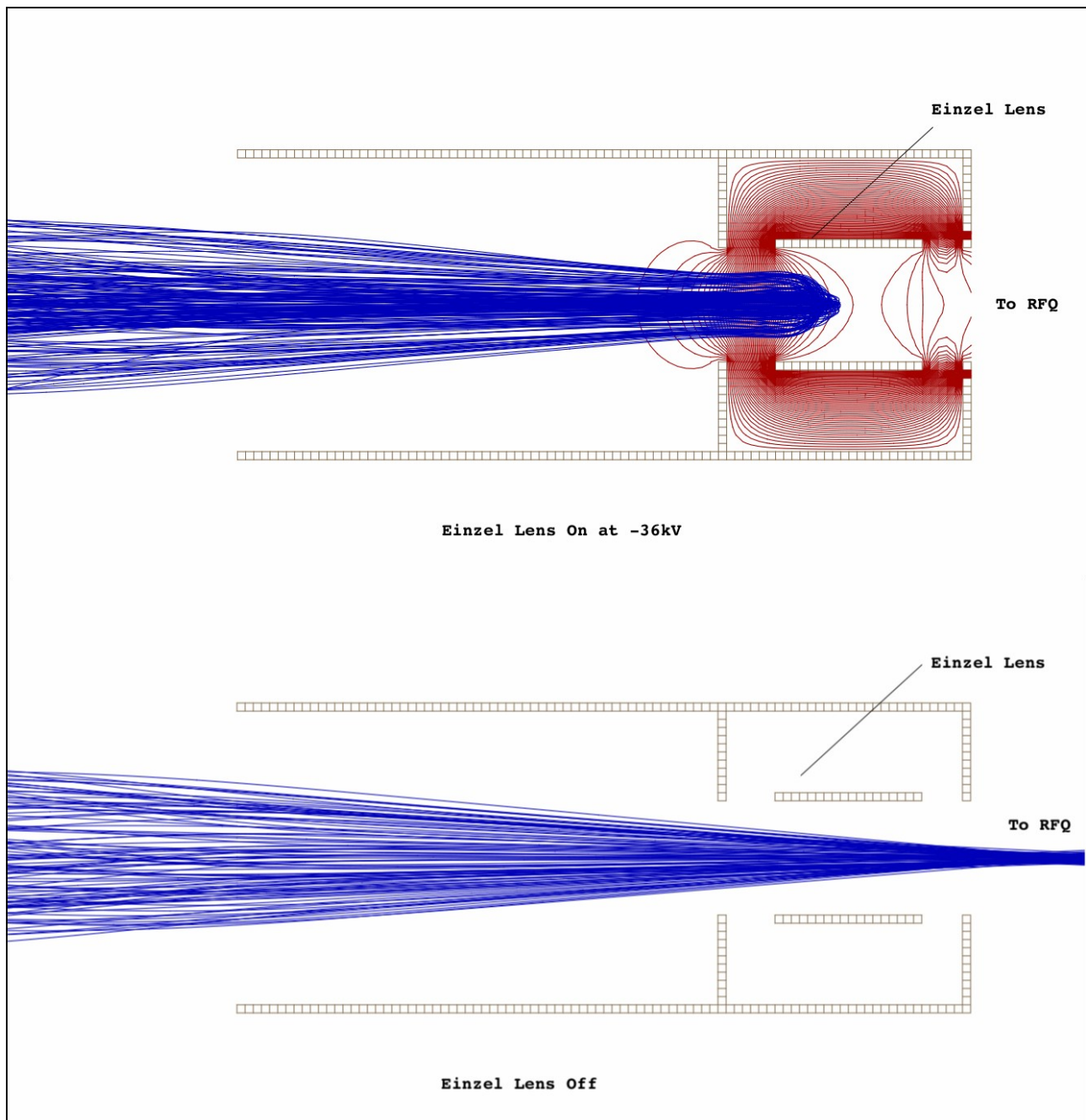


Figure 4.8: The magnetic field from the solenoid (See Figure 4.8) focuses the beam into the entrance of the RFQ when the Einzel lens is off. When the Einzel lens is on, it acts like a mirror on the H- beam by reflecting the beam away from the RFQ.

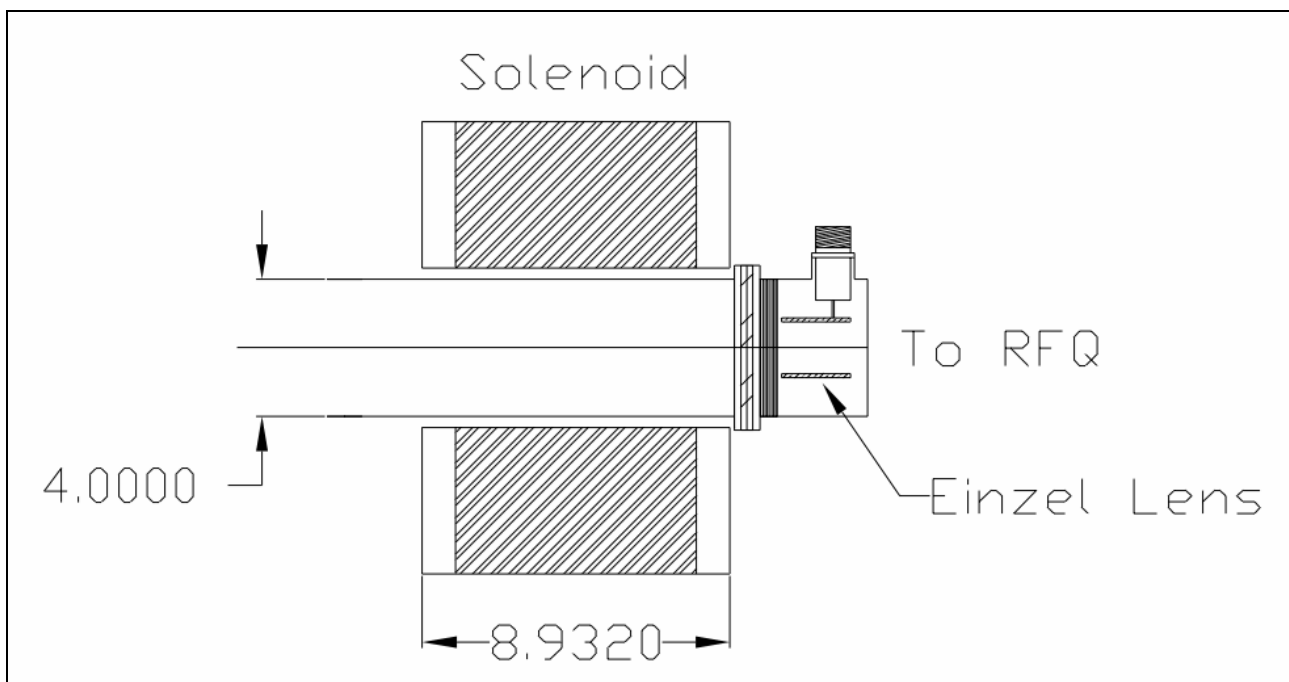


Figure 4.9: This is the zoomed in view of the LEBT just before the RFQ which shows how the the Einzel lens is mounted. (Designed by A. Markarov)

4.2.4.b. The Energy Pulser

The energy pulser works in a similar way as the Einzel lens except that it is built right into the H- source. Figure ?? shows a possible configuration where an inner electrode to -36.5 kV so that the potential difference between the source and the electrode is -1.5kV. This potential difference is sufficient to stop the H- ions from escaping the source.

4.3. The RFQ

The BNL RFQ model [10] was optimized with PARI to produce the RFQ model which is used in all the simulations of this report. PARI was set up to optimize the output energy to 753keV and to adjust the RFQ vane modulation only. The result is an RFQ with parameters summarized in Table 4.3. Some of these parameters are plotted in Figure 4.10. Using these parameters, a PARMTEQM simulation was set up to transport 10^4 particles from the entrance to the exit of the RFQ. For 50mA of H⁻, only 2% of the H⁻ ions are lost in the simulation. Figure 4.11 shows the result of the transport through the RFQ and Figures 4.12, 4.13 and 4.14 show the phase space and real space distributions of the particles before and after they have gone through the RFQ. The initial phase space distributions used in the simulation are from BNL (See the matching results at the entrance of the RFQ using Trace2D which is shown in Figure Error: Reference source not found) because the FNAL RFQ will be similar to the BNL RFQ.

Parameter	Value	Units
Input energy	35	keV
Output energy	753	keV
Frequency	201.25	MHz
Number of cells	147	
Length	162.95	cm
Minimum radial aperture	0.26	cm
Maximum peak surface field	21.45	MV/m
Peak cavity power ²	~100	kW
Duty factor (80 μ s, 15 Hz)	0.12	%
Design current	50	mA
Modulation m	$1 \leq m \leq 2.1$	
Intervane voltage	66.87	kV
Transmission efficiency	98	%
Input emittance (x,y)(norm, $1 \times$ rms)	0.3	$\pi \cdot \text{mm} \cdot \text{mrad}$
Output emittance (x,y) (norm, $1 \times$ rms)	0.3	$\pi \cdot \text{mm} \cdot \text{mrad}$

Table 4.3 The FNAL RFQ which has been optimized from the BNL RFQ model.

² BNL RFQ power requirement.

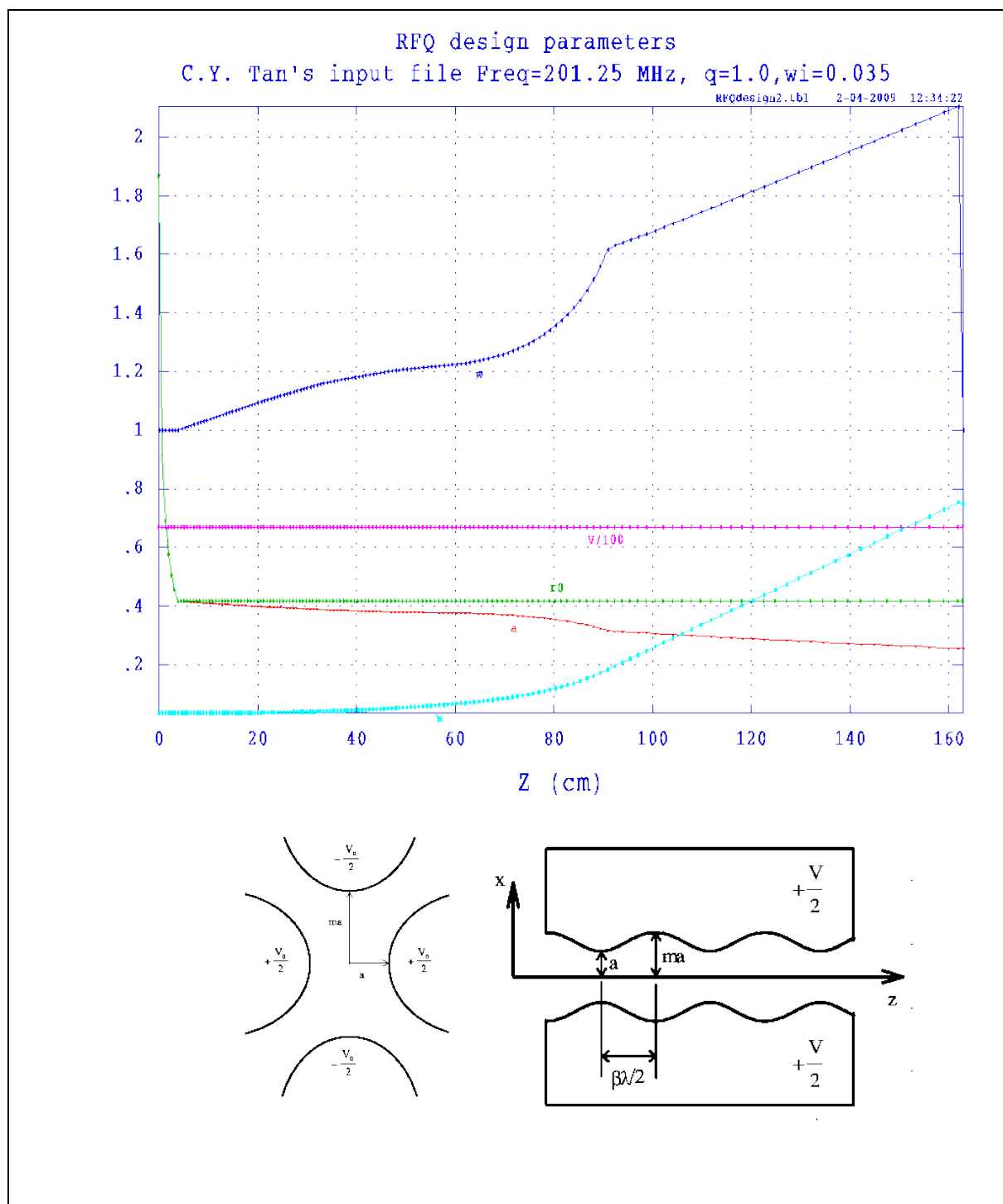


Figure 4.10: This is a plot of some of the RFQ parameters versus the length of the RFQ. a (cm, red) is the radius of the aperture, m (blue) is the modulation index, W (MeV, cyan) is the energy of the beam, $V/100$ (kV, magenta) voltage on the vanes divided by 100, and r_0 (cm, green) is the mid cell radial aperture. (Note: Bottom figure are Figures III-3 and III-4 of the PARMTEQM manual [13].)

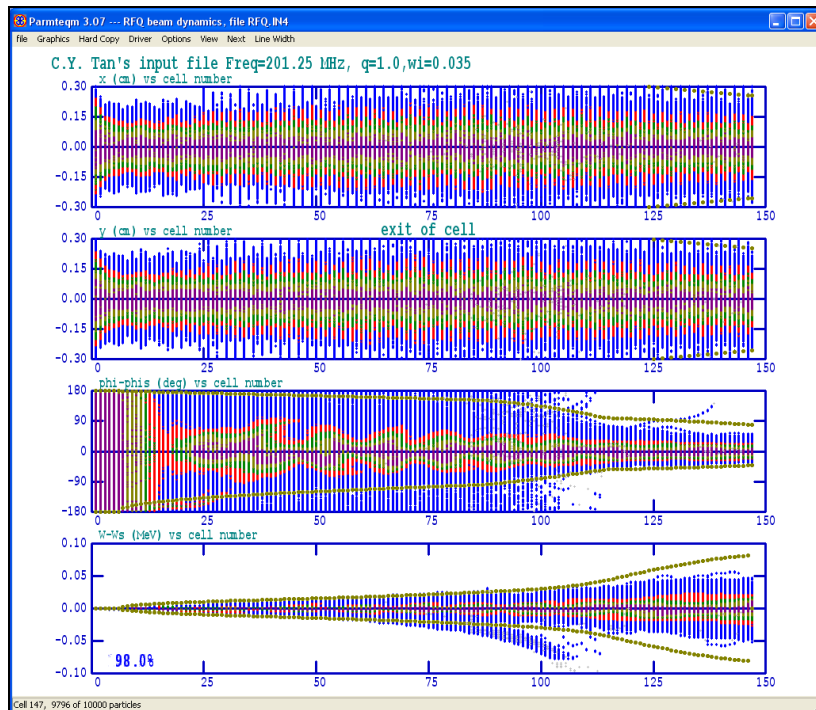


Figure 4.11: This is a PARMTEQM simulation of 50mA beam going through the RFQ. The transmission efficiency is 98%.

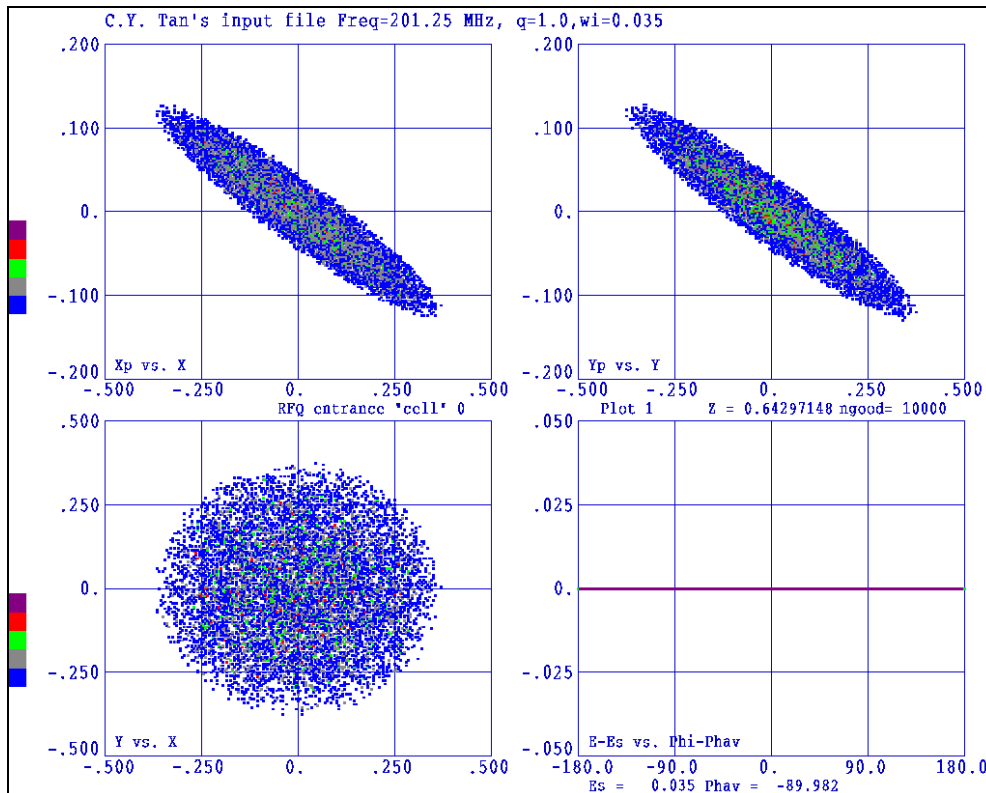


Figure 4.12: The initial phase space distribution at the entrance of the RFQ.

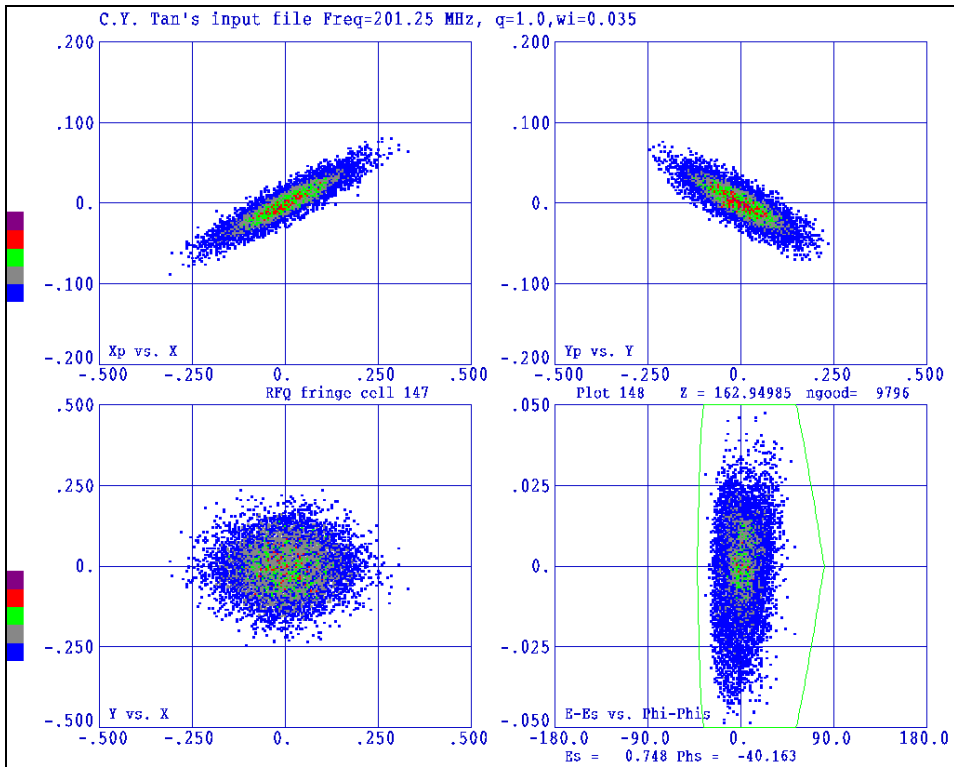


Figure 4.13: The phase space distribution at the end of the RFQ.

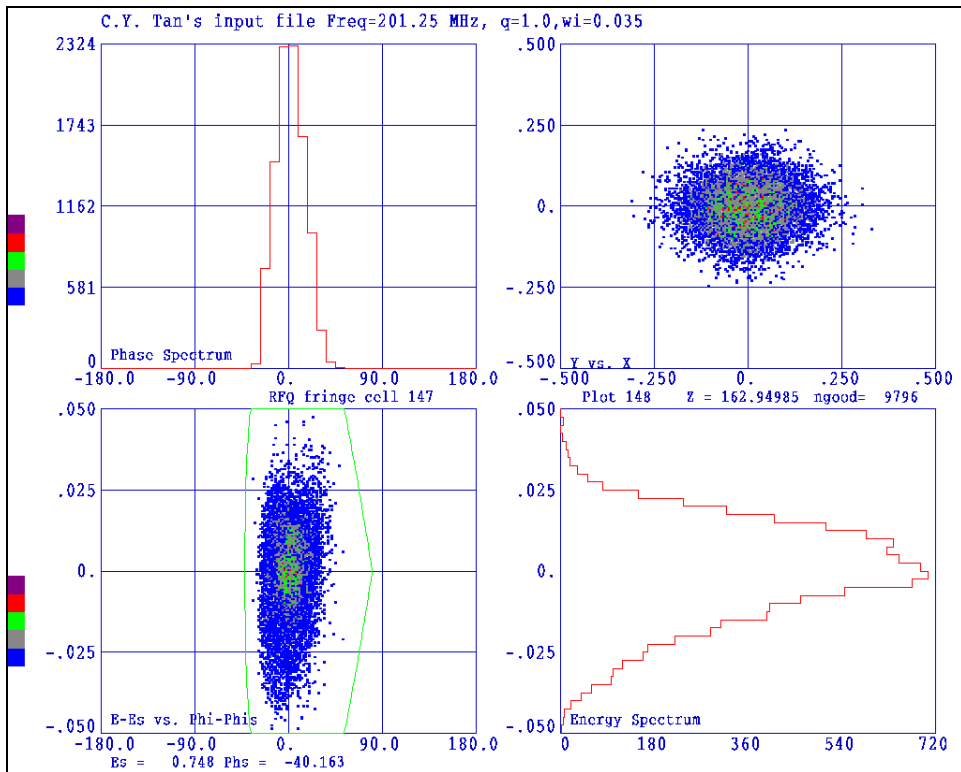


Figure 4.14: The longitudinal distribution at the end of the RFQ.

4.4. Optics for the MEBT

The plan is to use the present BNL MEBT as a prototype for the proposed MEBT. The MEBT contains 1 buncher and 3 quadrupoles for matching, 2 sets of steerers in both planes, 1 current transformer and 1 Faraday cup for diagnostics and a beam stop for safety. BNL has managed to squeeze all these parts into 73.25 cm of space. See Figure 4.15. The MEBT lattice which matches to the present DTL calculated using Trace3D is shown in Figure 4.16. Note: for the $\beta\lambda=60$ mm MEBT and so it is unrealistic to design the lattice with $\beta\lambda$ spacing because it is too short.

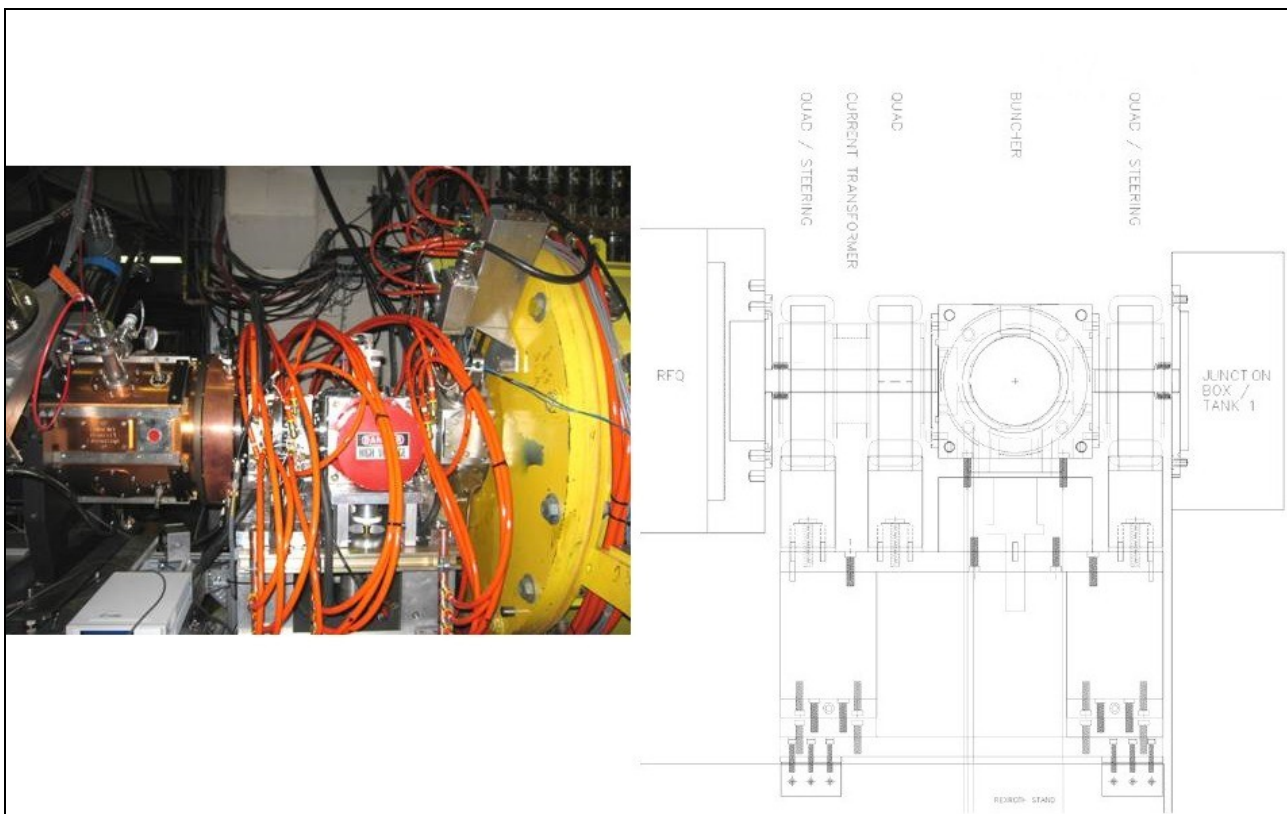


Figure 4.15: This is the BNL MEBT which only occupies 73.25 cm of space between the end of the RFQ and the start of the first DTL. (Pictures courtesy of D. Raparia)

4.4.1. Buncher

The buncher is a two gap cavity because a single gap cavity cannot fit in 70 cm of space. From Trace3D, the effective buncher gap voltage for each gap $E_0TL=34.5$ kV. is The peak voltage V_g across the gap of the buncher can be calculated by first calculating the peak E-field E_0 from the following formula

$$E_0 = \frac{E_0TL}{T \times L} \quad (4)$$

where L is the length of the RF gap and T the transit time factor (dimensionless). T is approximately given by the following

$$T = \frac{\sin\left(\frac{\omega_{RF} L}{\beta c 2}\right)}{\frac{\omega_{RF} L}{\beta c 2}} \quad (5)$$

where $\omega_{RF} = 2\pi \times f_{RF}$, and c is the speed of light. And so for an RF gap of $L = 1$ " and 750keV H-ions ($\beta = 0.04$), the transit time factor is calculated to be $T = 0.73$. Substituting these values into Eq. (4), $E_0 = 1.8$ MV/m and thus the peak gap voltage $V_g = E_0L = 47$ kV.

Parameter	Value	Units	Comments
Energy gain per unit charge E_0TL	34.5	kV	Calculated by Trace3D. See Figure 4.16.
Gap length L	1	inch	Assumption
Gap voltage V_g	47	kV	
Shunt impedance $R_s/2$	1	M Ω	Assumption
Transit time factor T	0.73		

Table 4.5 Single gap buncher parameters using $E_0TL = 34.5$ kV. For a double gap buncher, see text, Table 4.4 and Figure 4.16.

With this gap voltage it is possible to calculate the power requirements of the buncher if the shunt impedance R_s is first selected. A reasonable value for a copper cavity is $R_s/2 = 1$ M Ω for each gap and from the definition of shunt impedance, the average power loss from dissipation on the walls of the cavity P_D is [11] (Note: this definition takes into account the transit time factor T)

$$P_D = 2 \times (E_0TL)^2 / (R_s/2) = 2 \times (34.5 \times 10^3 [\text{V}])^2 / 10^6 [\Omega] = 2.4 \text{ kW} \quad (6)$$

The power transferred to the beam by a buncher in the ideal case is zero because the earlier half of the beam is decelerated while the latter half is accelerated equally and thus the total energy delivered is zero. However, in the worst case scenario, all the beam is accelerated and so the power P_b delivered to the beam is:

$$P_b = I_{\text{beam}} \times (2 \times E_0 TL) = (50 \times 10^{-3} [\text{A}]) \times (2 \times 34.5 \times 10^3 [\text{V}]) = 3.5 \text{ kW} \quad (7)$$

Therefore, the total power P_T required for the buncher is the sum of power lost from dissipation and the power delivered to the beam [12]

$$P_T = P_D + P_b = (2.4 + 3.5) \text{ kW} = 6.0 \text{ kW} \quad (8)$$

which is less than 8 kW of power available from the IPA RCA 7651 tube amplifier. Note: this calculation is an over-estimation of the required power for the buncher.

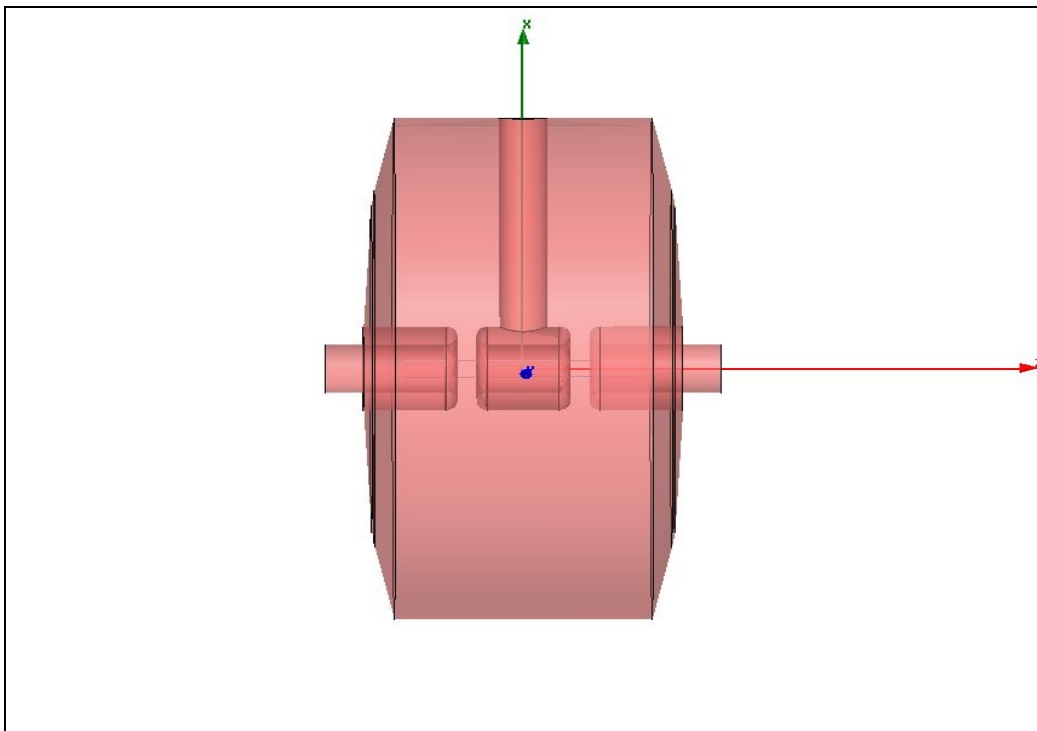


Figure 4.17: A two gap buncher design using HFSS which fits in the space requirement of the MEBT.

4.4.2. Quadrupoles

From the Trace3D calculations, the quadrupoles in the MEBT must have a gradient of at least 43.5 T/m and have a length of 45mm. See Figure 4.6 and Table 4.4. The quadrupole which will be used is a BNL design which is air cooled and is 45mm long. It has a maximum gradient of 65 T/m at 300A, for a pulse width of 500us at 6.4 Hz. This means that its duty factor is which is $(500 \mu\text{s} \times 6.4 \text{ Hz}) = 0.3\%$ about a factor of 2 higher than what is required for operations which is $(100 \mu\text{s} \times 15 \text{ Hz}) = 0.15\%$. Therefore, this quadruple design satisfies the MEBT requirements. Figure 4.18 shows the BNL a partially assembled BNL quadrupole and the end view drawing.

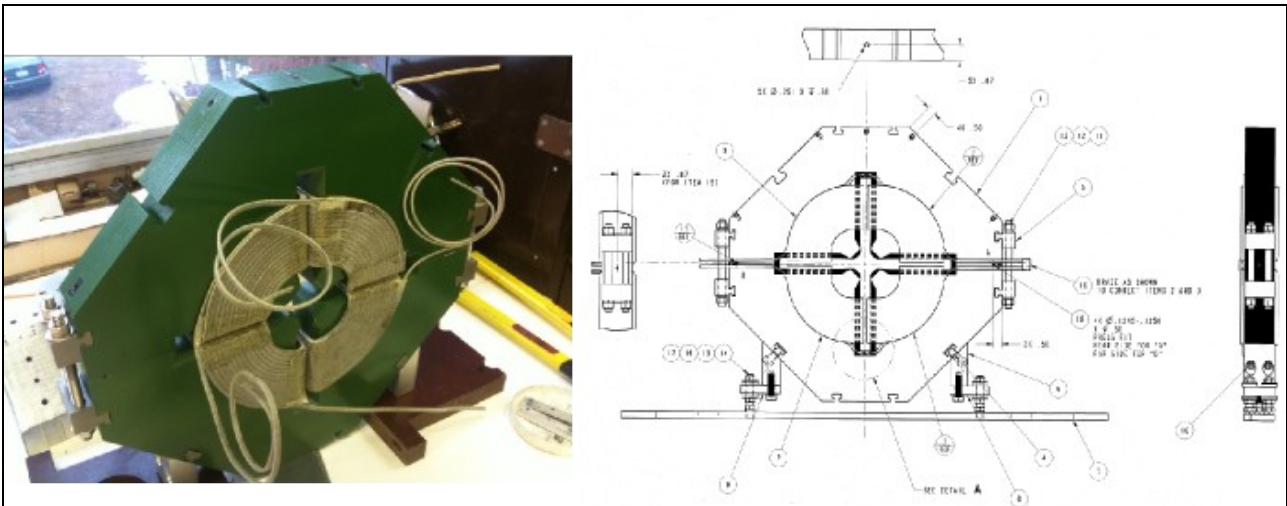


Figure 4.18: The BNL quadrupole partially assembled and the drawing of the quadrupole. This quadrupole design satisfies the operational requirements. (Photograph courtesy of M. Okamura)

4.5. Layout

The present layout of the H- and I- lines are shown in Figure 4.19. All the elements in the I-line upstream of the DTL will be removed for the installation of the proposed injector. The approximate space required for the proposed injector is drawn in shades of red on the floor plan of the pre-accelerator enclosures shown in Figure 4.20. It is clear from this figure that the proposed injector will occupy a lot less space than the existing injector.

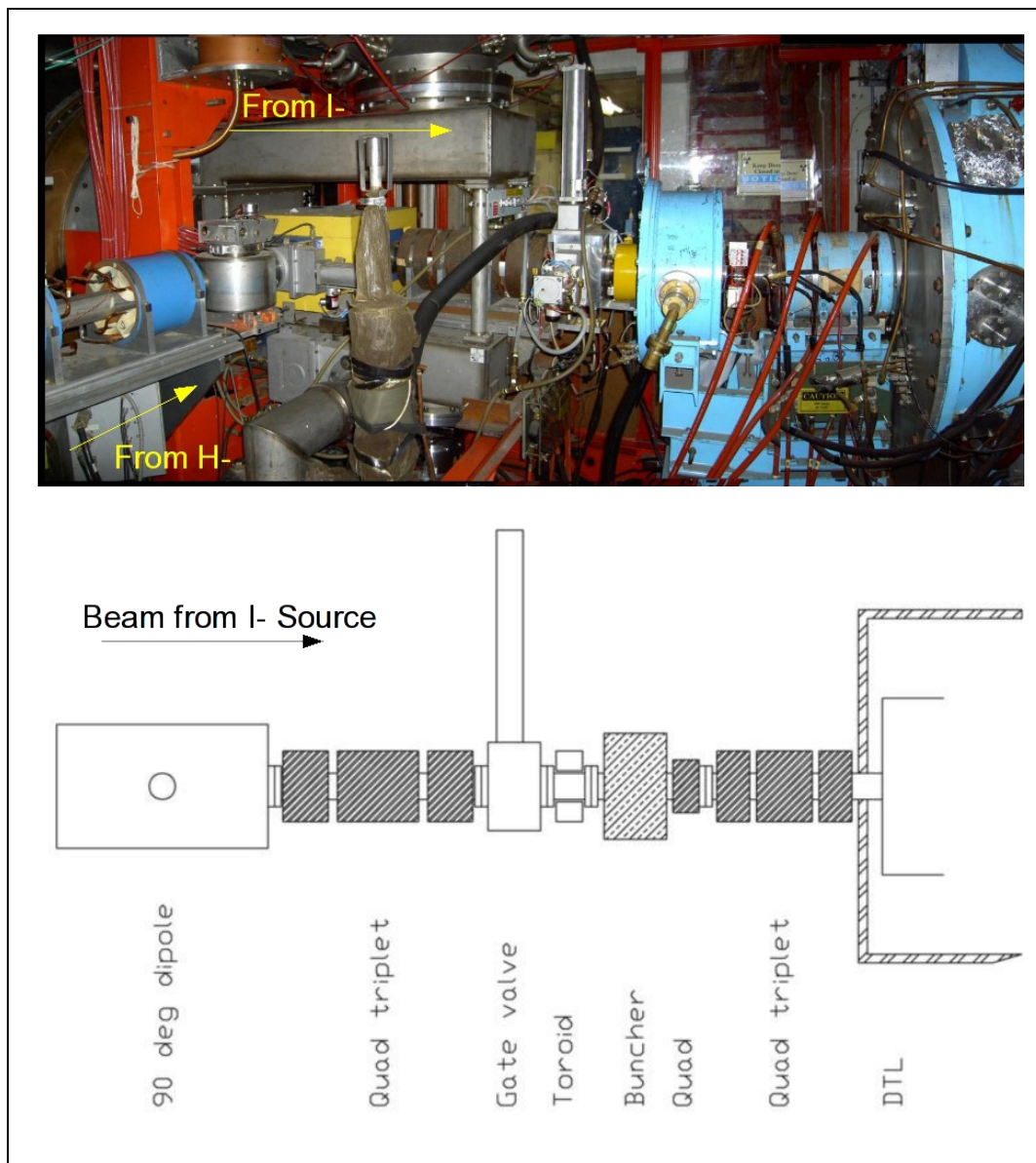


Figure 4.19: The photograph (composed from three photographs) in this figure shows the present I- and H- transport lines. The drawing below it shows the elements in the I- line. All the elements upstream of the DTL will be removed for the new injector installation.

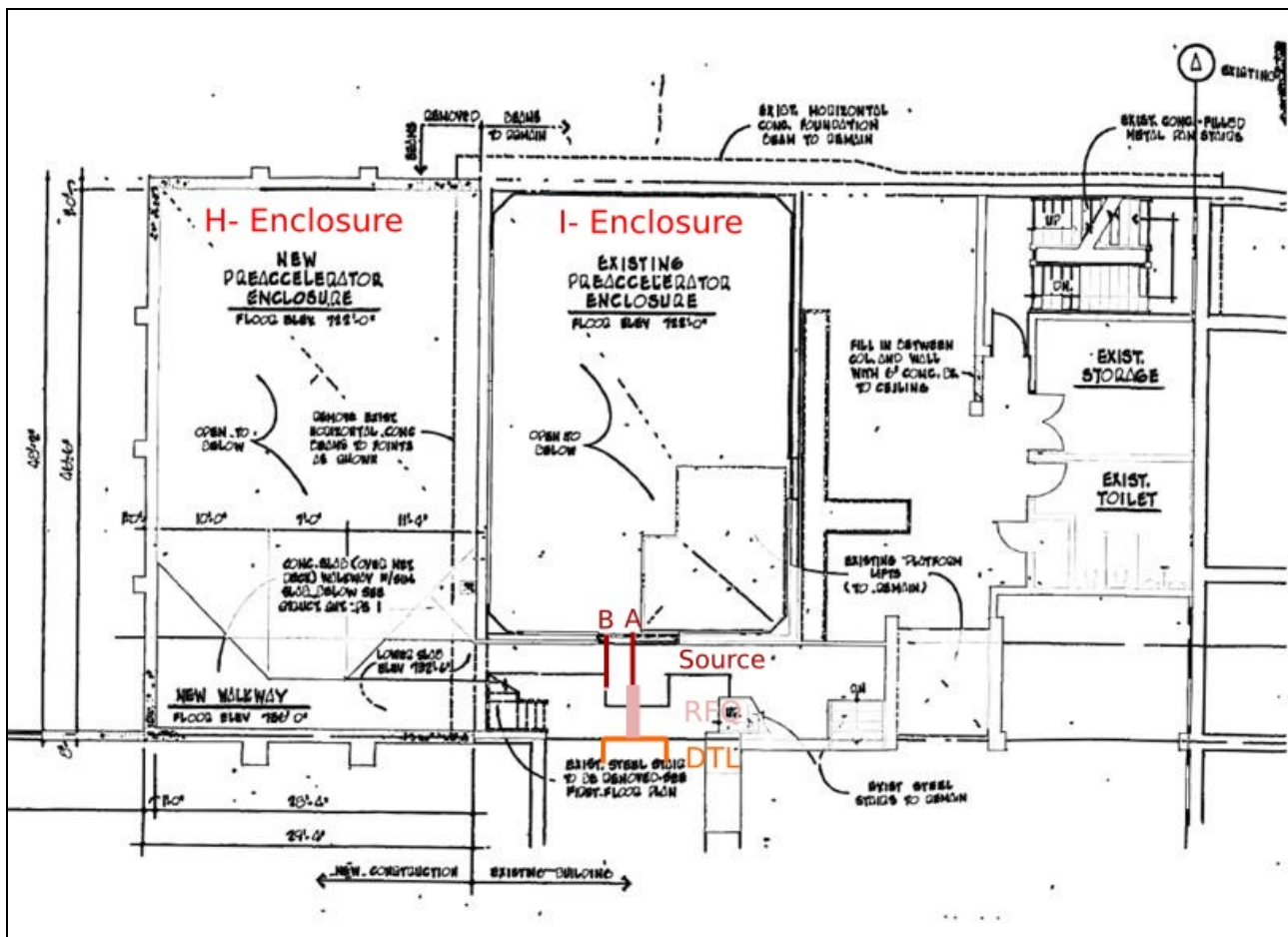


Figure 4.20: The floor plan of the existing pre-accelerator enclosures which house both the H- and I- sources. A sketch of the new injector is drawn in shades of red in this figure. Note: the length of the sketch is approximately to scale, but the width is not. It is clear that the proposed injector will occupy a lot less space than the present I- injector.

5. Performance Goals

The goal is to have an injector that performs as well as the present Cockcroft-Walton system. This means that:

1. The reliability and uptime of the proposed injector must be at least 97%.
2. The beam current at the end of the DTL 1 must be at least 37.5 mA. See Figure 5.1.

Table 5.2 shows the minimum beam current requirements at each stage of the proposed injector which will give the same beam current at the end of DTL 1 with the Cockcroft-Walton.

Location	Current (mA)	ϵ_x (norm., 1σ , $\pi \cdot \text{mm} \cdot \text{mrad}$)	ϵ_y (norm., 1σ , $\pi \cdot \text{mm} \cdot \text{mrad}$)	Comments
Start of DTL 1	46	0.86	0.91	Taken on 3 Jun 2009

Table 5.1 These are the present transverse and longitudinal emittances at the start of DTL 1 which the proposed injector must reproduce or improve upon.

Location	Current* (mA)	% Transmission from previous location	Comments
Output of H- source	60	-	Source can operate up to 100mA. See ref. [2].
End of LEBT before RFQ	50	84	See section 4.2.1.
End of RFQ	49	98	See section 4.3.
End of DTL 1	39.5	80	See section 4.4.

Table 5.2 These are minimum beam current requirements for the proposed H-injector which matches the present slit source+Cockcroft-Walton injector.*The definition of beam current is discussed in this section (Section 5.).

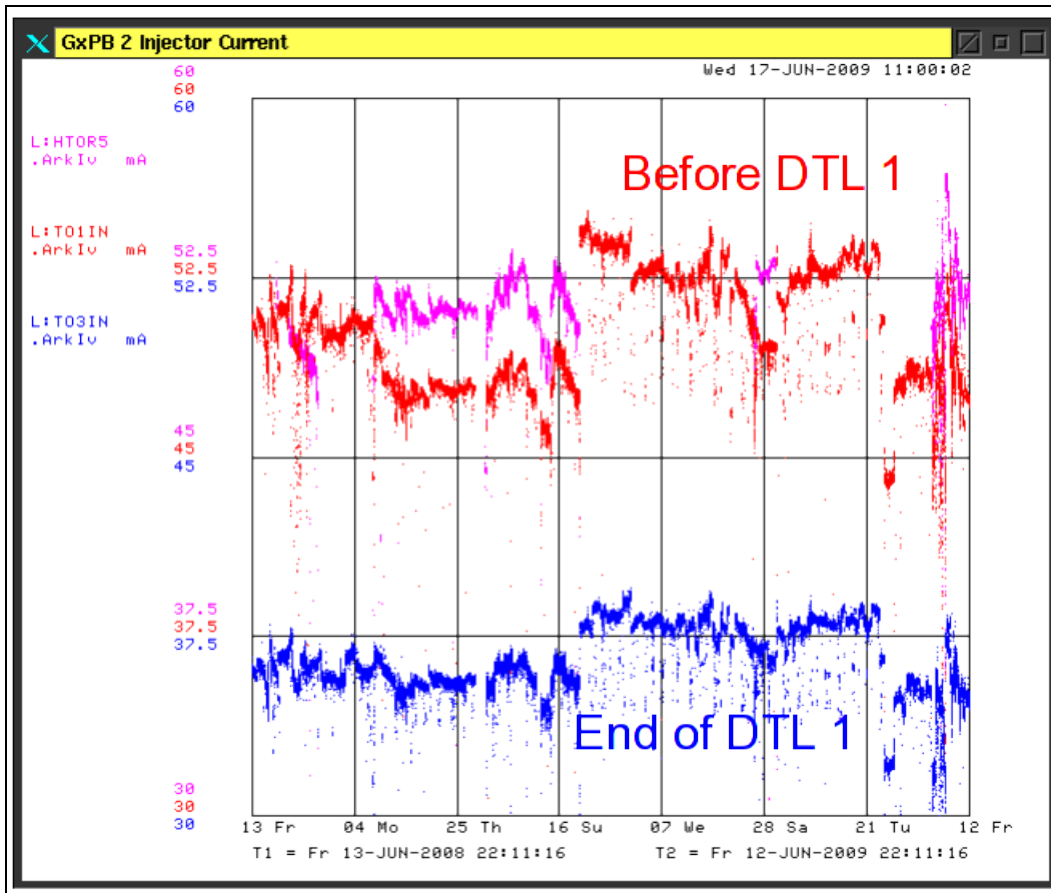


Figure 5.1: This figure shows the performance of the present injector for the past year. Maximum current at the end of the first DTL is about 37.5mA. The loss of H- by going through the DTL is about 30% because the beam in the MEBT is essentially DC and the tails are not captured in the DTL.

At the output of the H- source, the beam current I_s is defined to be

$$I_s = Q_s / T_s \quad (9)$$

where Q_s is the total charge at the output of the H- source and $T_s \approx 80 \mu s$ is the length of the pulse.

In the simulations which use either PARMTEQM [13] or PARMILA [14], the beam current I_{beam} is defined to be:

$$I_{\text{beam}} = qNf_{\text{bunch}} \quad (10)$$

where q is the charge per particle, N is the number of H- ions, f_{bunch} is the bunch frequency. In the simulations, it is assumed that $f_{\text{bunch}} = f_{\text{RF}} = 201.25 \text{ MHz}$ because all the adjacent buckets are filled in the $\sim 80 \mu s$ macro pulse. This means that if $I_s = I_{\text{beam}}$ there are no losses because a uniformly distributed Q_s decreases linearly as the size of the macro pulse is linearly shrunk from T_s to $1/f_{\text{RF}}$.

6. Cost Estimate

The cost of this plan is based upon either similar accelerator hardware which have been built or are being built. These costs have been summarized in Table 6.1. The cost estimate for the RFQ is from the LBNL physics group who have built or have designed several other RFQs and it is also the group who built the BNL RFQ. Their estimate which has been broken down in Table 6.2 can serve as a guide for the most cost effective solution for the completion of the project. Other material costs are based on recent projects and known inventory of the required hardware. It should be pointed out that:

1. Only the RFQ includes contingency.
2. The cost estimate does not include accelerator division labor costs.

The total cost so far is estimated to be approximately \$900k. At present, there is only one estimate for the RFQ, but a second estimate from LINAC systems has been requested and it is expected to be lower. If a contingency of 20% is included (which the RFQ estimate already includes) for materials the estimate is increased to about \$1.1 million.

Element	Quantity	Total Cost	Notes	Power	ps cost
Solenoid	3		BNL style: 2335 G, 241 mm	60Amp	4K
Quad #1	2	0 (Reuse Booster Quad)	.18T/m, 3 inch gap, 150mm long	40Amp	4K
Quad #2	1	0 (Reuse Booster Quad)	.16T/m, 3 inch gap, 150mm long	40Amp	4K
Dipole	1	0 (Reuse 8Gev Trim)	15T, 8 inch gap, 185mm	20Amp	2.5K
Vacuum Valve	3	12K	3 inch		
Beam Stop	1	0 (Reuse Present Stop)	3 inch		
Wire Scanner	1				
Toroid	3	0 (Reuse Present Toroids)	3 inch		
Buncher Cavity	1	40K	1.6 inch gap, 9 inches, 48KV	Reuse	
RFQ	1	700K (25 % contingency)	1 meter, 200 MhZ, ~100Kwatt	Reuse	
Trim	3	0 (Reuse Booster Trims)	6 inches, 15 T, 3 inch gap	20Amp	2.5K
Kicker	1	25K (Resuse Cer BP, Ferrite)	12 inches, 2 inch gap	Reuse	10K
Chopper	1	0 (Reuse present notcher)	8 inches, 2 inch gap	Reuse	5K
Misc Hardware		Beam Pipe/Flanges reuse			10K
Engineer	1	1 month	Stands, Vacuum, Kicker, Deb		50k
Cad Drawings	1	1 month	Stands, Vacuum, Kicker, Deb		50k
Mech Labor	2	3 months			50k
TOTAL		735K			90k
TOTAL		900K			

Table 6.1 The cost estimate for the materials of the project. There are no contingencies in the estimate except for the RFQ which has 25% contingency. The cost of the solenoids are not shown here. See text for details.

Table 6.1 lists all the planned hardware required for the upgrade. Notice that many of the smaller items are already on hand. The cost for assembling the RF source for the RFQ is not included because the plan is to reuse a 6544 tube test system. The cost of the tubes will be minimal because the project will use the weak tubes which have been removed from the low energy RF systems. There are only four devices which need to be built. They are:

1. An RFQ.

2. A buncher.
3. Two solenoids
4. A magnetic kicker.

If a decision is made to build a second source for the Y configuration, then an additional solenoid will be required. The cost estimates for the solenoids depend on whether the spare HINS solenoid (originally built for PET) can be used or new ones designed and built for approximately \$35k each. The cost of three solenoids at \$35k each have been included in the final cost but are not displayed in Table 6.1.

6.1. Cost of RFQ

Component/Task	Sr Mech Eng	ME Designer 1	ME Designer 2	Sr Scientist	Material	Fabrication	Mech Tech	Metrology/Align	Total
Conceptual Design and Analysis									
Physics Design				33.0					33.0
Conceptual Mechanical Design	27.7								27.7
Thermal/Structural Analysis	20.7								20.7
3D CAD Modeling			26.0						26.0
Detailed Design									
Detailed fabrication drawings									
RFQ Module		13.9	11.7						25.5
Support Structure		6.9	3.1						10.0
Tuners, sensors, fixtures, etc.		6.9	2.6						9.5
Engineering Effort		6.9	5.2						12.1
Develop specs and procedures	10.4								10.4
Detail design oversight	5.5								5.5
Internal Review									
Preparation	2.8		3.1						5.9
Review	1.4		1.0						2.3
Design Revisions	3.5	2.0	5.8						11.3
Documentation	13.8		10.4						24.2
Fabrication/Procurement									
Fabrication Oversight									
RFQ Module	17.3	34.7	10.4						62.3
Support Structure	2.1	5.8	1.6						9.4
Tuners, sensors, fixtures, etc.	4.1	11.6	2.6						18.3
Couplers, RF windows	1.8	5.3	1.2						8.3
Fabrication/Assembly									
RFQ Module					60.0	76.5	99.5	7.9	243.9
Support Structure					12.0	9.0			21.0
Tuners, sensors, fixtures, etc.					12.0	14.9			26.9
Couplers, RF windows					38.0	24.4	11.3		73.7
Vacuum (pumps, gages, manifolds)					0.0				0.0
RFQ Tuning and Testing	1.4		1.0	8.3					10.7
Total w/o Contingency									\$698.8k
Contingency (25%)									\$174.7k
Total w/Contingency									\$873.4k

Table 6.2 The broken down cost estimate for building an RFQ from the LBNL physics group. Note: the cost in green for a mechanical technician has been removed for the RFQ estimate shown in Table 6.1.

7. Conclusion

The injector is over 40 years old. The technology and knowledge required to maintain the systems is being lost either to obsolescence or retirement. The cost of actual parts is relatively small compared to other linac systems but when the cost of downtime and manpower is included the new RFQ injector system will quickly pay for itself. The cost of approximately 40 hours of downtime/year and the labor required to keep the system not only running but up to the required operational beam parameters is estimated to be at \$400k/year on average.

This plan will use many of the parts which are already on hand and mature technologies which the lab is familiar with, for example, the H- magnetron source. A new RFQ will need to be built, but its specifications are well within the present technical expertise of industry and should present very little technical risk. Therefore, it is expected that the new injector will work as reliably as the BNL injector.

This plan also assumes that the amount of manpower to maintain the injector will be reduced from the present two senior techs, one junior tech, one tech assistant and one operational specialist mentioned in subsection 3.3. The time and effort required to operate and tune the present H-sources, Linac and the Booster to an acceptable level is difficult to assign a cost value. But this cost is non-negligible because the present system has and will continue to be a major source of instability and downtime. This plan presents a design that will not only pay for itself in a matter of two to three years but will also improve the beam quality for all the downstream users. The implementation of the new system is estimated to take about one year. If this plan is approved and its implementation is started now (Fall 2009), installation can occur in the Spring of 2011.

8. Acknowledgments

The authors would like to thank:

1. The BNL linac group: J. Alessi, D. Raparia and V. Lodestro who graciously hosted three of the authors (Bollinger, Schmidt and Tan) in the fall of 2008 for a tour of the BNL injector and who gave them much of the information used in this plan.
2. D. Raparia (BNL) who generously supplied the BNL LEBT and MEBT design which served as the base line design in this plan.
3. M. Popovic (FNAL) who supplied both the present DTL PARMILA model used in the simulations and the data for the cost estimate.
4. W.M. Tam (FNAL) for calculating the required angle for the magnetic kicker in the first version of the plan.

A.1. The BNL Injector

The BNL injector will be discussed in the following two subsections. The reason for this discussion is because the BNL injector was upgraded from a nearly identical FNAL style slit source and Cockcroft-Walton in the fall of 1988 to a round source+RFQ. The motivation for doing the replacement at BNL came from the expectation of “improved reliability, simpler maintenance, and the added convenience of having the ion source located at nearly ground potential” [15]. These are the same technical reasons for upgrading the FNAL Cockcroft-Walton system to an RFQ system.

The round source+RFQ which has been operational at BNL since then, has operating parameters which are nearly identical to the FNAL requirements and so a direct comparison between the two can be made. The operational experience of the BNL round source+RFQ has been very positive and thus an upgrade of the FNAL injector to this configuration should carry very little technical risk.

A.1.1. The BNL Injector (1982-1989)

The BNL injector switched to H⁻ operation in 1982 [2]. The 750keV injector is nearly identical to the present FNAL 750keV injector except that it has only one slit source+Cockcroft-Walton while FNAL has two slit source+Cockcroft-Waltons. The injector typically runs at a repetition rate of 6.6-7.5 Hz with a pulse width of about 500 μ s. The current at the output of the Cockcroft-Walton is about 40-50 mA [16]. The beam is then accelerated and either injected into the Booster or switched into a second beam line for isotope production.

A.1.2. The BNL Injector (1989-present)

BNL built a round source+RFQ injector which replaced the one slit source+Cockcroft-Walton in 1989. The typical running parameters of the round source are shown in Table A 1.1. This can be compared to the typical running parameters of the slit source shown in Table 3.3 and it is clear that the BNL round source is operating at about 25% lower power than the FNAL slit source. When operating at this power, the single BNL H⁻ source has been “very reliable, operating continuously for ~6 months, with essentially no parameter adjustments required once the source is stabilized.” [2].

There has been a number of reconfigurations of the LEBT and MEBT at BNL. The present configuration [3] is shown in Figure A1.1. The length of the LEBT for the unpolarized, high intensity H⁻ source is about 4 m because it is constrained by the position of the polarized H⁻ source. In order to get maximum transmission of the H⁻ beam from the source to the RFQ, Xe gas focusing must be employed. There is a 30% improvement of the transmission of H⁻ beam in the LEBT with Xe gas focusing compared to without gas focusing. However, gas focusing does strip the H⁻ beam and causes a loss of 32% of the beam in the LEBT (gas stripping has been discussed in section 4.2.1.).

The LEBT transports the H⁻ beam to the RFQ. The RFQ is about 1.5m long and accelerates the 35keV beam from the source to 750keV. The RFQ has not had any problems since its installation [17].

The 750keV beam is transported to the DTL through the MEBT. The length of the MEBT

has been shortened to 70 cm from the previous configuration of about 7 m. The new MEBT has greatly reduced the losses (essentially zero), transmission and emittance of the beam at the end of the DTL. The improvements are about a factor of 2 smaller in emittance in both planes compared to the previous configuration and a transmission efficiency of between 65 – 70% compared to the previous configuration of 50 – 55% [3].

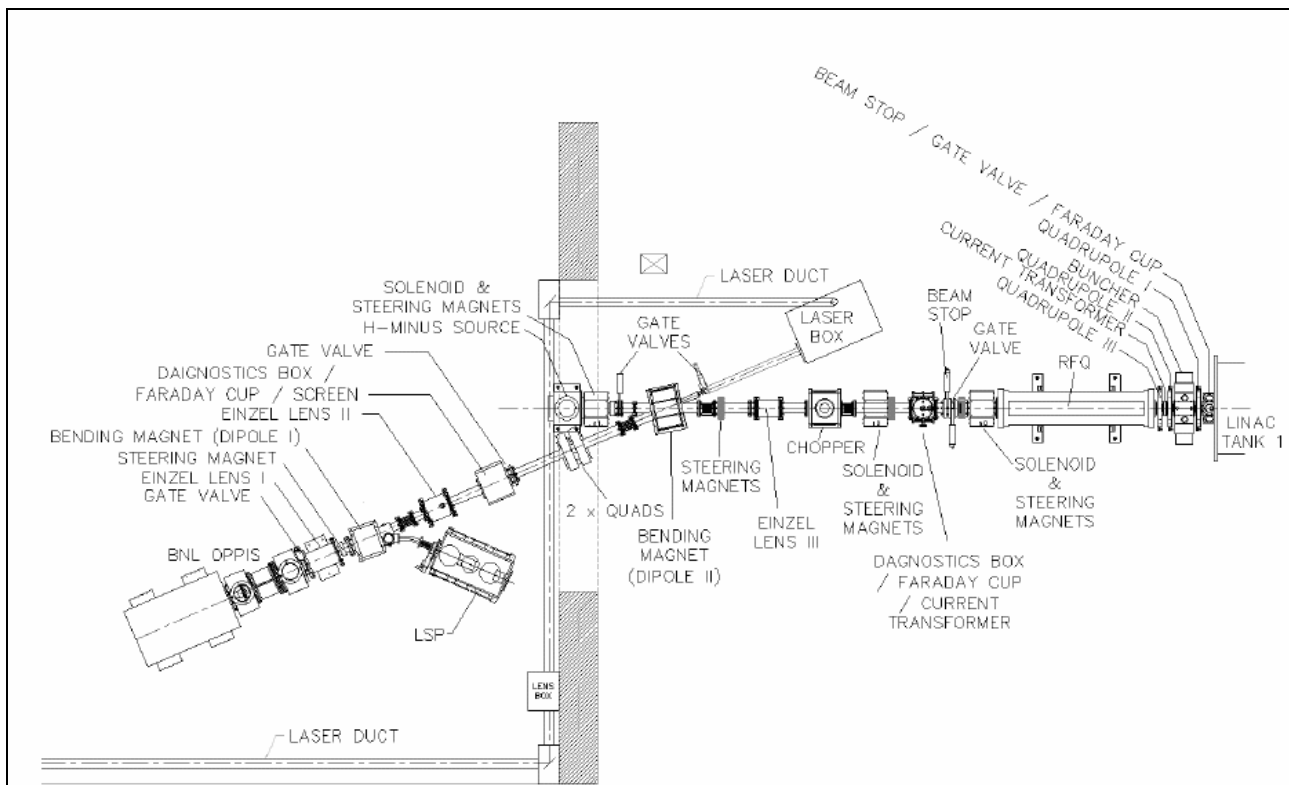


Figure A1.1: This is the BNL injector (as of 2009 [3]) which has a H-magnetron source and a polarized H- source. The MEBT, which is after the RFQ and before Linac Tank 1 is only 73.25 cm long, contains 1 buncher, 3 quadrupoles, 2 sets of horizontal and vertical steerers (not shown in drawing), 1 current transformer and 1 beam stop/gate valve/Faraday cup package. Figure 4.15 is a picture of the MEBT. (Picture courtesy of D. Raparia)

Parameter	Value	Units
H- current	90 – 100	mA
Current density	1.5	A/cm ²
Extraction voltage	35	kV
Arc voltage	140 – 160	V
Arc current	8 – 18	A
Repetition rate	7.5	Hz
Pulse width	700	μ s
Duty factor	0.5	%
rms normalized emittance	~0.4	$\pi \cdot \text{mm} \cdot \text{mrad}$
Cs consumption	< 0.5	mg/hr
Gas flow	~2	sccm
Average power	$150 \text{ V} \times 13 \text{ A} \times 5 \text{ Hz} \times 600 \mu\text{s} \approx 6$	W

Table A1.1 Some BNL H- round source parameters copied from Ref. [2].

References

- [1] C.W. Schmidt & C.D. Curtis, "A 50-mA Negative Hydrogen Ion Source", IEEE Proc. Nucl. Sci., NS-26, pg. 4120-4122, 1972.
- [2] J.G. Alessi, "Performance of the Magnetron H- Source on the BNL 200MeV Linac", AIP Conf. Proc., Vol. 642, pg. 279-286, 2002.
- [3] D. Raparia, et al, "Results of LEBT/MEBT Reconfiguration at BNL 200 MeV Linac", Part. Acc. Conf. Proc., , , 2009.
- [4] J.G. Alessi et al, "H- Source and Low Energy Transport for the BNL RFQ Preinjector", AIP Conf. Proc., Vol. 210, pg. 711-716, 1990.
- [5] R. Webber, "H- Ion Source Requirements for the HINS R&D Program", , Beam docs 3056v1, 2008.
- [6] M. Reiser et al, "Theory and Design of Charged Particle Beams", 2nd Ed., pg. 243-254, Wiley-VCH, 2008.
- [7] J.P. Carneiro, "H- Stripping Equations and Application to the High Intensity Neutrino Source", Beam docs 2740.
- [8] J.F. Williams, "Single and Double Electron Loss Cross Section for 2-50-keV H- Ions Incident upon Hydrogen and the Inert Gases", Phys. Rev., Vol. 154, No. 1, pg. 9-12, 1967.
- [9] S.N. Kaplan, et al, "Electron Detachment from 20-MeV D- Ions by a Magnetic Field", Phys. Rev., Vol 131, No. 6, pg. 2574-2577, 1963.
- [10] D. Raparia, Private Communication, 2009.
- [13] K.R. Crandall et al, "RFQ Design Codes", 11, LA-UR-96-1836, 2005.
- [11] D.A. Edwards & M.J. Syphers, "An Introduction to the Physics of High Energy Accelerators", , pg. 24-28, John Wiley & Sons, 1993.
- [12] T.P. Wangler, "RF Linear Accelerators", 2nd Ed., pg. 42-43, Wiley-VCH, 2008.
- [14] H. Takeda, "Parmila", pg. 15, LA-UR-98-4478, 2005.
- [15] J.G. Alessi et al, "Performance of the New AGS RFQ Preinjector", Part. Acc. Conf., , pg. 999-1001, 1989.
- [16] R.L. Witkover, "Operational Experience with the BNL Magnetron H- Source", AIP Conf. Proc., Vol. 111, pg. 398-409, 1984.
- [17] J. Alessi, Private Communication, 2008.